

Optimal Scheduling of Industrial Combined Heat and Power Plants under Time-sensitive Electricity Prices

Sumit Mitra*, Lige Sun[†], Ignacio E. Grossmann^{*‡}

December 24, 2012

Abstract

Combined heat and power (CHP) plants are widely used in industrial applications. In the aftermath of the recession, many of the associated production processes are under-utilized, which challenges the competitiveness of chemical companies. However, under-utilization can be a chance for tighter interaction with the power grid, which is in transition to the so-called smart grid, if the CHP plant can dynamically react to time-sensitive electricity prices.

In this paper, we describe a generalized mode model on a component basis that addresses the operational optimization of industrial CHP plants. The mode formulation tracks the state of each plant component in a detailed manner and can account for different operating modes, e.g. fuel-switching for boilers and supplementary firing for gas turbines, and transitional behavior. Transitional behavior such as warm and cold start-ups, shutdowns and pre-computed start-up trajectories is modeled with modes as well. The feasible region of operation for each component is described based on input-output relationships that are thermodynamically sound, such as the Willans line for steam turbines. Furthermore, we emphasize the use of mathematically efficient logic constraints that allow solving the large-scale models fast. We provide an industrial case study and study the impact of different scenarios for under-utilization.

1 Introduction

The simultaneous generation of heat and power (cogeneration) is not only energy-efficient and reduces CO₂ emissions, but it also helps to increase the

*Center for Advanced Process Decision-making, Department of Chemical Engineering, Carnegie Mellon University, Pittsburgh, PA 15213

[†]RWTH Aachen University, Aachen, Germany

[‡]Corresponding author. Email address: grossmann@cmu.edu

robustness of the energy infrastructure by means of decentralized generation. Compared to the generation of heat and power in separate facilities, efficiency improvements between 10% and 40% can be observed (Madlener and Schmid, 2003) [1]. With applications in industrial processes, district heating and micro generation, cogeneration is recognized to be a “proven, reliable and cost-effective” (International Energy Agency report (Kerr, 2008) [2]) energy option, “deployable in near term” (Oak Ridge National Lab report (Shipley et al., 2008) [3]).

The impact of cogeneration is also acknowledged by policy makers. The G8 Summit Declaration (June 2007) [4] suggests “adopting instruments and measures to significantly increase the share of combined heat and power (CHP) in the generation of electricity.” An example of a such a policy can be found in the European Union, where the CHP Directive (Directive 2004/8/EC, 2004) [5] sets a framework to promote growth of CHP, which has since been adopted in national laws, e.g. in two steps in Europe’s largest energy market, Germany. First, the Integrated Energy and Climate Programme of the German Government (Meseberg, 2007) [6] defines a target of 25% for CHP generation by 2020. Second, the Combined Heat and Power Act (KWKG, 2009) [7] outlines feed-in conditions for CHP generation. In the meanwhile, the share of CHP in electricity generation has risen from 9.3% (2004) to 13% (2009) in Germany (Eurostat, 2012) [8]. According to a report and individual country scorecards prepared by the International Energy Agency (Kerr, 2008) [2], a large potential for future CHP developments can be observed throughout the world, especially in the US and in developing economies such as India and China.

Many of the CHP plants are industrial CHP plants that supply steam and power to energy-intensive processes, e.g. pulp and paper mills, aluminum plants, refineries and other chemical processes. These CHP plants are usually run by the companies themselves or by on-site utility providers. In 2010, as a result of the recession, many of these production facilities were under-utilized; the capacity utilization in pulp and paper mills in the US was at 83.1% and in aluminum plants at 68.6% (capacity utilization for primary metals, Federal Reserve data, March 2011) [9]. In fact, the US is not the only place where under-utilization impacts competitiveness. In the example of Germany, the chemical companies reside in chemical parks, where multiple companies run their operations to take advantage of economies of scale, e.g. in utilities (CEP, October 2011) [10]. An A.T. Kearney study (Lewe and Disteldorf, 2007) [11] reveals that, among other issues, only 50% of the estate is utilized at some sites, even in a pre-recession setting. A subsequent survey (Lewe and Schroeter, 2010) [12] confirms that “the pressure is still on”.

Fortunately, under-utilization can be a chance for tighter interaction with the power grid, which is in transition to the so-called smart grid. De-regulation and an increasing share of renewable energies lead to more

variability in time-sensitive electricity prices, offering potential incentives for industrial sites as producers and consumers if they are able to cope with the fluctuations (Wassick, 2009 [13]; Samad and Kiliccote, 2012 [14]). Therefore, it is essential to characterize the flexibility of a CHP plant and use the obtained insights to determine how to dynamically respond to the time-sensitive electricity prices.

In the following, we will answer three main questions related to the decision-making for CHP plants under time-sensitive electricity prices:

1. Is it technically and economically feasible to operate an under-utilized CHP plant flexibly in interaction with the smart grid?
2. How large can the potential economic gains be, i.e. what is the optimal way to operate?
3. How can these plants be modeled such that the process flexibility is captured appropriately?

For this purpose, we address the operational optimization of CHP plants by first reviewing existing approaches in the chemical engineering, power systems and energy research community in section 2. We then develop a generalized mode model for plant components that explicitly considers flexibility with respect to the feasible region of operation and dynamic behavior in section 3 and 4. Next, we provide an industrial case study that can be solved efficiently despite the large computational model in section 5. Finally, we draw conclusions in section 6.

Additionally, if the production facility has flexibility itself to optimize energy consumption it might be worthwhile to integrate the operational decision-making of the CHP plant with that of the production facility. This scenario is especially feasible if the CHP plant is owned by the same company as the production facility. Todd et al. (2009) [15] discuss the benefit of such an approach for aluminum production and Agha et al. (2010) [16] study the joint scheduling of a batch plant and a CHP plant using a MILP model. Note that the resulting formulation can be nonlinear, depending on the nature of the industrial process. Furthermore, it is possible to enhance flexibility by investments in thermal storage systems, as it is explored for district heating (Christidis et al., 2012) [17] and for industrial CHP (Cole et al., 2012) [18]. CHP plants can also be part of so-called virtual power plants that facilitate the integration of different renewable energy sources (Wille-Hausmann et al., 2010) [19]. Additional benefits might be realized by interacting with power reserve markets (Lund et al., 2012) [20]. However, in this paper, we focus on the derivation of an efficient MILP model for the operational optimization of CHP plants with given steam and electricity demand profiles according to time-sensitive electricity prices.

2 Literature Review

Past work on the modeling of CHP plants, mostly in the chemical engineering community, addresses the design of utility systems. Approaches based on thermodynamic targets and heuristic rules (Nishio et al., 1980) [21], optimization models (e.g. the LP model by Petroulas and Reklaitis (1984) [22]), as well as combinations thereof (Marechal and Kalitventzeff, 1998 [23]) are used for this purpose. Papoulias and Grossmann (1983) [24] introduce a MILP formulation for selecting the equipment from a superstructure. For a fixed superstructure, Colmenares and Seider (1989) [25] solve an NLP for the integrated design of a utility plant and a chemical plant. The model of Papoulias and Grossmann (1983) [24] is refined by Bruno et al. (1998) [26] who provide a MINLP formulation that considers nonlinear characteristics such as steam properties, efficiencies, and gas enthalpies in combustion turbines. Iyer and Grossmann (1998) [27] use a linear multi-period design and operation formulation to account for variable operating conditions. Based on the concept of the Willans line (Willans, 1888) [28], which relates the steam flowrate with the power output of a turbine, different formulations are proposed to account for part load behavior within the design problem in more detail (Mavromatis and Kokossis, 1998 [29]; Varbanov et al., 2004 [30]; Aguilar et al., 2007 [31]). Furthermore, the concept of the Willans line is extended to gas turbines. These papers also follow the multi-period approach to address variability in operating conditions on a design level, but do not consider the operational problem on a short-term basis either.

Multi-period models that address the operational planning of CHP plants without inter-temporal constraints include the work of Micheletto et al. (2008) [32] as well as Luo et al. (2012) [33]. Micheletto et al. (2008) [32] describe a modified version of the model by Papoulias and Grossmann (1983) [24] for the operational planning of the CHP plant of a Brazilian refinery. Luo et al. (2012) [33] consider the environmental impact of a Chinese CHP plant based on a model that follows the Willans line approach.

For the short-term scheduling of CHP plants, one of the first rigorous MILP approaches can be found in Seeger and Verstege (1991) [34]. Salgado and Pedrero (2008) [35] review different modeling approaches and find the data-driven approach by Makkonen and Lahdelma (2006) [36] to be the most generic one. Makkonen and Lahdelma (2006) [36] represent the feasible region of operation of an entire CHP plant by a convex combination of extreme points in the space of heat output, power output and cost. Tina et al. (2012) [37] model the CHP plant of an Italian refinery based on data regression with polynomial functions and consider compliance to the European directive 2004/74/EC that defines requirements and benefits for cogeneration.

There are publications that combine a data-driven approach with logic constraints and start-up costs, i.e. model the unit commitment of the indi-

vidual components in more detail. For the long-term planning of a district heating network, Thorin et al. (2005) [38] use a similar approach as Makkonen and Lahdelma (2006) [36] to describe the operating regimes of the individual components and additionally include minimum up- and downtime constraints. In a similar manner, Christidis et al. (2012) [17] study the impact of heat storage in the context of the long-term planning problem.

An alternative approach to data-driven models is based on thermodynamic balance equations for each individual component in the CHP plant. While the corresponding mass balance for each component is linear, the respective changes in enthalpy are generally nonlinear. Therefore, equipment efficiencies can be nonlinear, which can be addressed with three main strategies.

First, the efficiency is assumed to be constant which might be reasonable depending on the component performance (Marshman et al., 2010) [39]. Second, the efficiency is approximated with a piece-wise linear function (Dvorak and Havel, 2012) [40]. Third, thermodynamic insights, such as the Willans line, are used to describe the component on an input-output basis (Ashok and Banerjee, 2003) [41]. It is important to note that the choice can be made for each component individually and researchers often combine the three approaches (Yusta et al., 2008 [42]; Agha et al., 2010 [16]; Velasco-Garcia et al., 2011 [43]). In the following, we describe the aforementioned papers that use thermodynamic balance equations in more detail.

Ashok and Banerjee (2003) [41] use the concept of the Willans line according to Mavromatis and Kokossis (1998) [29] and solve a case study in the Indian petrochemical industry. However, their formulation is nonlinear due to a quadratic objective and bilinear terms that result from multiplications with binary variables. Yusta et al. (2008) [42] study the economic impact of energy exchange with the Spanish power grid for a cogeneration system consisting of a gas turbine and a steam turbine using a piece-wise linear approximation for the gas turbine and a constant efficiency model for the steam turbine. Marshman et al. (2010) [39] employ a constant efficiency model for steam turbines and boiler to optimize the cogeneration facility of a paper and pulp mill. Agha et al. (2010) [16] integrate the scheduling of a co-generation facility into the resource task network formulation (RTN) that has been used for the scheduling of manufacturing facilities (Pantelides, 1994) [44]. They use piece-wise linear approximations for boiler efficiencies and constant steam turbine efficiencies. Velasco-Garcia et al. (2011) [43] utilize a simplified version of the model by Varbanov et al. (2004) [30] based on the Willans line approach to model the turbines of an industrial CHP plant and also incorporate a few logic constraints. However, they only consider the next set point for the CHP plant, i.e. their model looks only one time step ahead. Recently, Dvorak and Havel (2012) [40] model a district heating plant with piece-wise linear functions and account for minimum up- and downtimes.

The solution of the resulting optimization problems for CHP plants can be challenging. Dotzauer (1999) [45] uses a Lagrangean relaxation-based heuristic to solve the operational optimization of a CHP plant that also has a thermal storage. In subsequent publications, Lahdelma and co-workers extend their original formulation and include restrictions on minimum up- and downtime (Rong et al., 2009) [46]. They show that the problem can be solved with customized heuristic methods based on Lagrangean relaxation and dynamic programming. A MILP-based heuristic, which decomposes the problem into a sequence of optimization problems that sequentially optimize electricity, heat production and economic dispatch, is developed by Sandou et al. (2005) [47].

Restrictions like minimum up- and downtimes, that are modeled in some of the previously mentioned publications, complicate the formulation and originate from the so-called unit commitment problem (UC). Likewise, the power systems community studied different approaches to address the UC problem, such as genetic algorithms, dynamic programming and Lagrangean relaxation as well as mathematical programming (MILP). For a detailed review we refer to the papers by Padhy (2004) [48], and Sen and Kothari (1998) [49]. As noted by Hedman et al. (2009) [50], nowadays, MILP is the method of choice for practitioners due to advances in solution algorithms and computing power.

One common MILP formulation for the UC is provided by Arroyo and Conejo (2000) [51]. Carrion and Arroyo (2006) [52] propose an alternative formulation that reduces the number of binary variables. Hedman et al. (2009) [50] study the tightness for different formulations of logic constraints in the UC and explain why the formulation of Rajan and Takriti (2005) [53] is the tightest. Ostrowski et al. (2012) [54] show computational evidence that the original formulation by Arroyo and Conejo (2000) [51] has performance advantages. Furthermore, they give a formulation that tightens the ramp rate constraints. Recently, Simoglou et al. (2010) [55] develop an UC formulation that explicitly accounts for the different phases during start-up and shutdown of units. Their formulation also includes different start-up procedures such as hot, warm and cold start-ups.

It is important to note that the unit commitment literature usually considers “units” at a plant level, which means that the interactions of components within the plant are not modeled. Therefore, Cohen and Ostrowski (1996) [56] introduce the concept of operating modes that helps modeling the characteristics of “certain types of generating units”, which have additional ways of operating beyond just “on” or “off”. Cohen and Ostrowski (1996) [56] give the following examples of operating modes: combined cycle operation, fuel switching/blending, constant/variable pressure for turbines, overfire and dual boilers. Furthermore, they show that transitions between modes can be expressed as modes themselves. They use a dynamic programming approach to solve the resulting optimization problem.

To overcome the limitations of classical UC formulations for a tightly integrated power plant like a CCCT (combined cycle combustion turbine) plant, Lu and Shahidehpour (2004, 2005) [57], [58] model the inherent process flexibility with a mode model on a plant level, also using a dynamic programming/ Lagrangean decomposition framework. Liu et al. (2009) [59] provide a MILP model based on the level of individual components and show with a case study that it is superior to an aggregated mode model for the scheduling of CCCT plants due to the more accurate description of the physical range of operation.

Mitra et al. (2012) [60] use a mode model to optimize the operation for continuous power-intensive processes under time-sensitive electricity prices in the following two ways: an aggregated mode model is used for air separation plants and individual plant components are modeled for cement plants (grinder).

In this work, we propose a generalized mode model on a component basis for combined cycle CHP plants. The mode formulation tracks the state of each plant component in a detailed manner, and can account for different operating modes and transitional behavior. Different operating modes include fuel-switching for boiler, supplementary firing for gas turbines and variable operating pressure for steam turbines. Transitional behavior such as warm start-ups, cold start-ups, shutdowns and pre-computed trajectories during start-ups is modeled. The feasible region of operation for each component is described based on input-output relationships that are thermodynamically sound, such as the Willans line for steam turbines. Furthermore, we emphasize the use of mathematically efficient logic constraints that allow to solve efficiently the potentially large-scale models. We also provide an industrial case study, and study the impact of different scenarios for under-utilization.

3 Generic Problem Statement

Given is a combined heat and power (CHP) plant with a set of plant components $c \in C$ (steam turbines, gas turbines with heat recovery steam generators, boilers) that can produce the utilities $p \in P$: electricity (EL) and steam at different pressure levels (HP , MP , LP and CON (condensate)) as shown in Fig. 1. The CHP plant has to satisfy hourly demand of electricity and steam. Surplus electricity can be sold to the power grid and electricity can also be purchased during hours of underproduction. The electricity prices vary on an hourly basis $h \in H$ and it is assumed that a forecast is available.

The problem is to determine modes of operation for each plant component and their respective production levels of steam and electricity. On a plant level, sales and purchases of electricity as well as overall steam production have to be determined, so that the given demand is met on an hourly

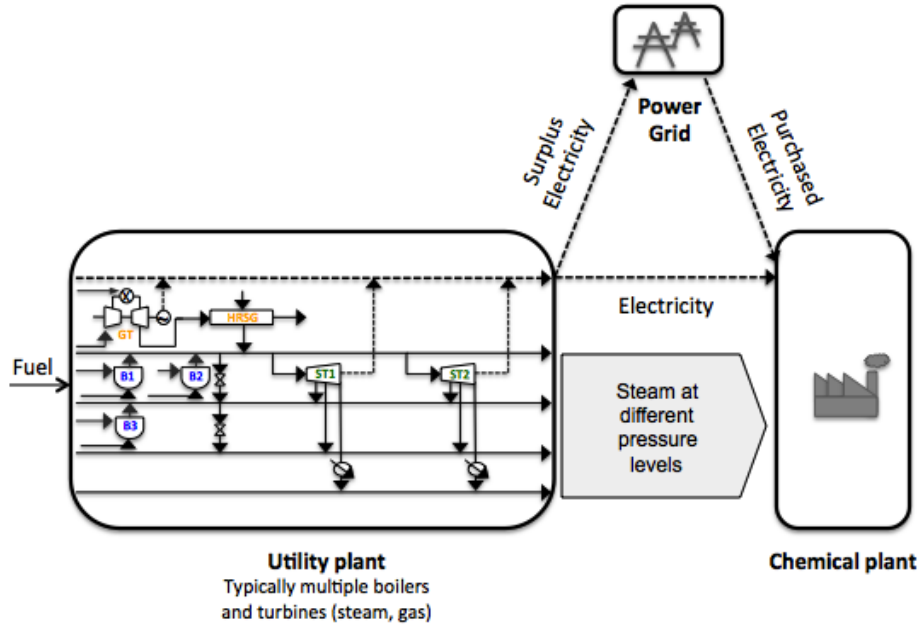


Figure 1: **Visualization of the problem statement: superstructure of utility plant**

basis. The objective is to maximize the CHP plant's profit.

4 Model Formulation

The application of a mode model requires two major set of constraints for each plant component (boilers, gas turbines and steam turbines as shown in Fig. 1). First, the modes and the corresponding operating regions have to be described for each component. Second, transitions between modes and operational restrictions have to be defined. Additionally, mass balances for steam headers, demand constraints, further operational restrictions as well as representations for revenue and costs have to be included on a plant level.

4.1 Production Modes and Feasible Region

In this section, we first describe the general formulation for the feasible region of operation. The formulation is based on the idea of representing the feasible region in the projected space of utilities. Thereafter, we customize the linear formulation for each plant component in a way that implicitly accounts for nonlinear efficiencies.

Each component $c \in C$ of the CHP plant has a set of discrete operating

modes $m \in M_c$, e.g. "off", "production", "warm start-up" and "cold start-up" (see nomenclature section). In every time period (hour h), only one mode can be active, which is described with the disjunctive constraint (1). The binary variable $y_{c,m}^h$ defines the term that applies in the disjunction.

For each component c , the feasible region of operation is defined in terms of continuous variables $Pr_{c,p}^h$ for all utilities $p \in P$: electricity (EL) as well as steam at different pressure levels, HP , MP , LP and CON (condensate). $x_{c,m,i,p}$ are the extreme points i of mode m of component c in terms of the utilities p . These extreme points have to be determined a-priori, which we will describe later for each component individually. The convex combination of the extreme points, with weight factors $\lambda_{c,m,i}^h$, defines the production $Pr_{c,p}^h$ at hour h for each component c and utility p .

$$\bigvee_{m \in M_c} \left(\begin{array}{l} \sum_{i \in I} \lambda_{c,m,i}^h x_{c,m,i,p} = Pr_{c,p}^h \quad \forall p \\ \sum_{i \in I} \lambda_{c,m,i}^h = 1 \\ 0 \leq \lambda_{c,m,i}^h \leq 1 \\ y_{c,m}^h = 1 \end{array} \right) \quad \forall c \in C, h \in H \quad (1)$$

The disjunction (1) is reformulated using the convex hull (Balas (1985) [61]) to allow for solving the program with an MILP solver. The convex hull reformulation can be written with constraints (2) - (7). Note that $\bar{M}_{c,m,p}$ is the maximum production of product p in mode m .

$$\sum_{i \in I} \lambda_{c,m,i}^h x_{c,m,i,p} = \bar{P}r_{c,m,p}^h \quad \forall c \in C, m \in M_c, p \in P, h \in H \quad (2)$$

$$\sum_{i \in I} \lambda_{c,m,i}^h = y_{c,m}^h \quad \forall c \in C, m \in M_c, h \in H \quad (3)$$

$$0 \leq \lambda_{c,m,i}^h \leq 1 \quad \forall c \in C, m \in M_c, i \in I, h \in H \quad (4)$$

$$Pr_{c,p}^h = \sum_{m \in M_c} \bar{P}r_{c,m,p}^h y_{c,m}^h \quad \forall c \in C, p \in P, h \in H \quad (5)$$

$$\bar{P}r_{c,m,p}^h \leq \tilde{M}_{c,m,p} y_{c,m}^h \quad \forall c \in C, m \in M_c, p \in P, h \in H \quad (6)$$

$$\sum_{m \in M_c} y_{c,m}^h = 1 \quad \forall c \in C, h \in H \quad (7)$$

In the following, we explain for each component $c \in C$ what the different operating modes $m \in M_c$ are, and how the feasible region in terms of constraints (2) - (7) can be described.

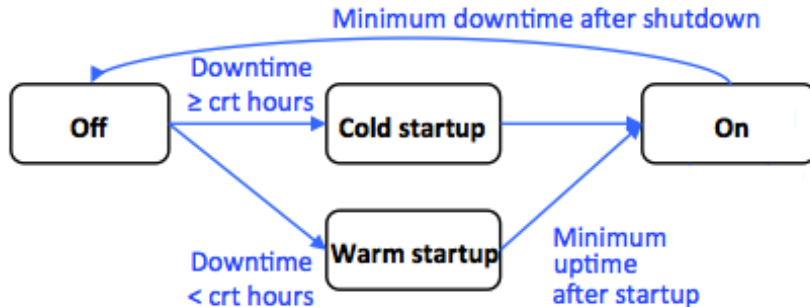


Figure 2: State graph representation of a steam turbine.

4.1.1 Steam Turbines

Steam turbines expand pressurized steam to a lower pressure level and use the extracted mechanical energy to drive an electricity generator or to satisfy shaft demand. There are three main types of turbines: back pressure units, condensing units and extraction units. The operating modes for steam turbines can be classified into three categories: off mode, production mode and transitional modes.

For industrial CHP plants, most steam turbines only have one production mode since the operating pressure and temperature of inlet as well as outlet streams are fixed. Note that it is also possible to operate steam turbines in a variable pressure control mode with lower generation (Ostrowski and Cohen, 1996 [56]), which is done for large turbines in power plants. In this setup, the turbine’s rotor life is increased due to less temperature variation across the load range, but the ramping ability decreases since the steam pressure is controlled by the firing rate of the steam generator (Drbal et al., 1996 [62]). Examples of transitional modes include startup and shutdown procedures, which might vary depending on the turbine’s downtime and the corresponding temperature decrease.

The state graph of a steam turbine can be seen in Fig. 2. Each node represents the state (mode) of the equipment. The edges represent the direction of the allowed transitions and show the operational constraints. In the example in Fig. 2, the steam turbine has four operating modes: “off”, “warm start-up”, “cold start-up” and “on”. The start-up procedure depends on the downtime of the steam turbine. If the turbine was offline for more than crt hours (critical downtime), the turbine needs longer to heat up again. At the same time, the startup procedure is slightly different, mainly to ensure that the thermal stress limits of the turbine are not violated. Furthermore, the turbine has to follow minimum downtime and minimum uptime restrictions. We will discuss the modeling of transitional modes and

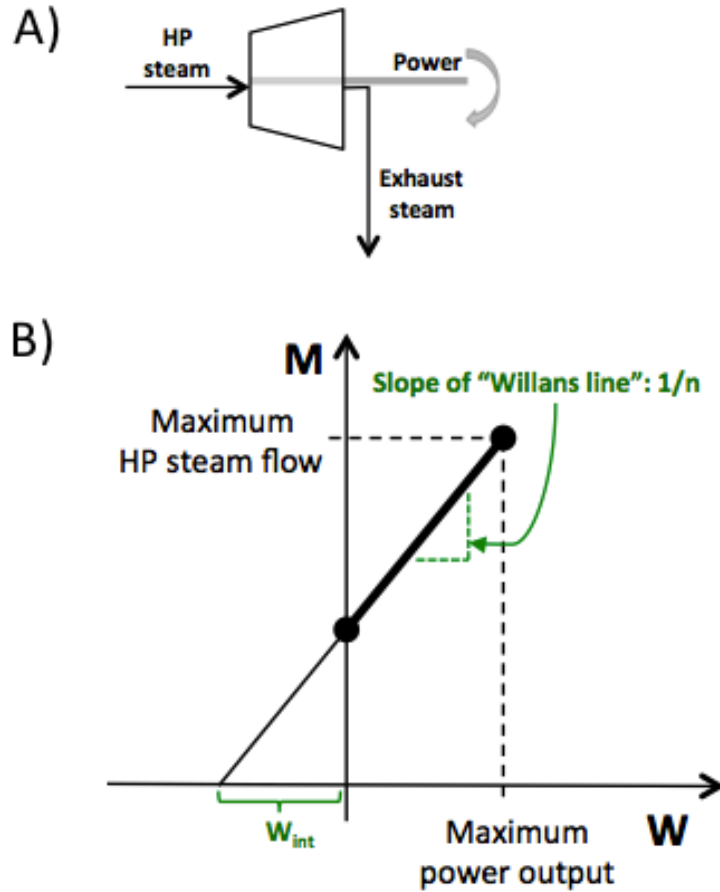


Figure 3: **A:** Conceptual representation of a single-stage steam turbine. **B:** Willans line relationship for a single-stage steam turbine in mode “on”.

associated logic constraints later in this paper.

4.1.1.1 Single-stage Steam Turbine Single-stage turbines can be classified as condensing and back pressure turbines. While condensing turbines expand the steam into a partially condensed state, back pressure turbines expand the steam to a pre-defined pressure at which it is still superheated. The conceptual representation of a single-stage steam turbine is depicted in Fig. 3-A.

The relationship between power output and steam flowrate can be expressed with a linear equation, the so-called Willans line (Willans, 1888 [28]). In equation (8), W is the power output and M the steam flow through the turbine. The parameters n and W_{int} stand for the slope and the intercept

of the Willans line, respectively.

$$W = nM - W_{int} \quad (8)$$

The extreme points $x_{c,m,i,p}$ (here: c=single-stage turbine and m=production) that are used within constraints (2)-(7) for the production mode would be the pair of steam output and power output for minimum and maximum production as shown in Fig. 3-B.

The Willans line is applicable for both type of turbines, although the individual fit coefficients take different values depending on the type and turbine size (Mavromatis and Kokossis, 1998 [29]; Varbanov et al., 2004 [30]; Aguilar et al., 2007 [31]). It is important to note that the Willans line, although being linear, accounts for nonlinear variations in turbine efficiency, assuming that efficiency losses are a fixed percentage of the maximum power output (Mavromatis and Kokossis, 1998 [29]). The aforementioned publications propose different derivations based on the maximum power output, the change in isentropic enthalpy, and the saturation temperature difference to obtain the actual coefficients for the Willans line equation. It is important to note that for a given steam turbine with fixed operating conditions for inlet and outlet streams, the Willans line can easily be determined from operating or manufacturer data instead of performing thermodynamic calculations.

4.1.1.2 Multi-stage Steam Turbine Multi-stage turbines mostly have one high-pressure inlet stream, which is then expanded in a series of stages to intermediate pressure levels. In the last step, the steam is usually condensed. At each intermediate pressure level it is possible to remove steam from the turbine, which is called extraction if the extraction pressure is controlled and bleeding if it is not. In Fig. 4-A, the conceptual representation of a two-stage turbine with extraction is shown.

Similar to a single-stage turbine, a multi-stage turbine can also be described with the idea of the Willans line. As a result, the so-called “extraction diagram” can be constructed, which is a convex region described by linear constraints. In the following, we will describe how the extreme points $x_{c,m,i,p}$ (here: c=multi-stage turbine and m=production) that are used within constraints (2)-(7) of this diagram are obtained.

Multi-stage turbines can be decomposed into a cascade of individual single stage turbines (Mavromatis and Kokossis, 1998 [29]). For a turbine with n expansion stages, the first $n - 1$ stage can be described by a series of back pressure turbines and the n^{th} stage corresponds to a condensing turbine. Ashok and Banerjee (2003) [41] as well as Valesco-Garcia et al. (2011) [43] use the individual Willans line coefficients for turbines with (multiple) extraction streams and obtain a set of linear equations.

In other words, the example of Fig. 4-A could be represented by two Willans lines, one for each stage with a feasible region according to Fig. 3-B.

But what happens if we plot the combined feasible region of steam input-power output for the two stages? Assuming that the maximum flowrate of the first stage is greater or equal to the one of the second stage, we obtain a feasible region according to Fig. 4-B.

The line A-B represent the line of no extraction flow with the combined Willans line slopes of the individual stages. In contrast, the line D-E corresponds to full extraction of the inlet steam and therefore, the slope of the Willans is that of the first stage. The line B-C also has the Willans line slope of the first stage, because the flow through the second stage (exhaust flow) is at its maximum and only the flow through the first stage varies. The resulting diagram is also known as “extraction diagram”, and it is usually provided by the steam turbine manufacturer and commonly used in industry (e.g. Jacobs and Schneider, 2009 [63]).

Each pair of steam input-power output values within the feasible region has a corresponding pair of extraction and exhaust flow values. Due to the implied mass balance, it is possible to describe the feasible region only in the utility space of extraction flow, exhaust flow and power. Note that the feasible region is convex in the product space due to the linear nature of the Willans line equations and mass balances are preserved.

In this work, we exploit the convexity property and use the extreme points of the “extraction diagram” within equations (2)-(7). The approach is easily extendible to a larger number of pressure levels.

Aside from manufacturer data or analytical Willans line coefficients, we can obtain the extreme points also from historical operating data or steady-state simulation, knowing that the underlying governing equations are the Willans lines for each stage. Given a set of operating points, the extreme points of the convex hull can be determined with the quickhull algorithm (Barber et al., 1996 [64]) that is implemented for instance in MATLAB R2010a [65].

In the context of district heating CHP plants, Lahdelma and co-workers also use the idea of describing the feasible operation region with a convex hull (Makkonen and Lahdelma, 2006 [36]; Rong et al., 2009 [46]). However, they represent an entire CHP plant with the convex of combination of triplets: power output, heat output and cost. In contrast, Thorin et al. (2005) [38] and Christidis et al. (2012) [17] model district heating CHP plants on a component-basis. They describe the feasible region of steam turbines in the power output-heat output space (for a single pressure level) with linear inequalities based on operating data. Since the polyhedral representation of the feasible region can always be transformed from linear equations and inequalities (half-space representation) to a convex hull of points (vertex representation), using a tool like PORTA (Christof and Lobel, 1997 [66]), we see our approaches as comparable.

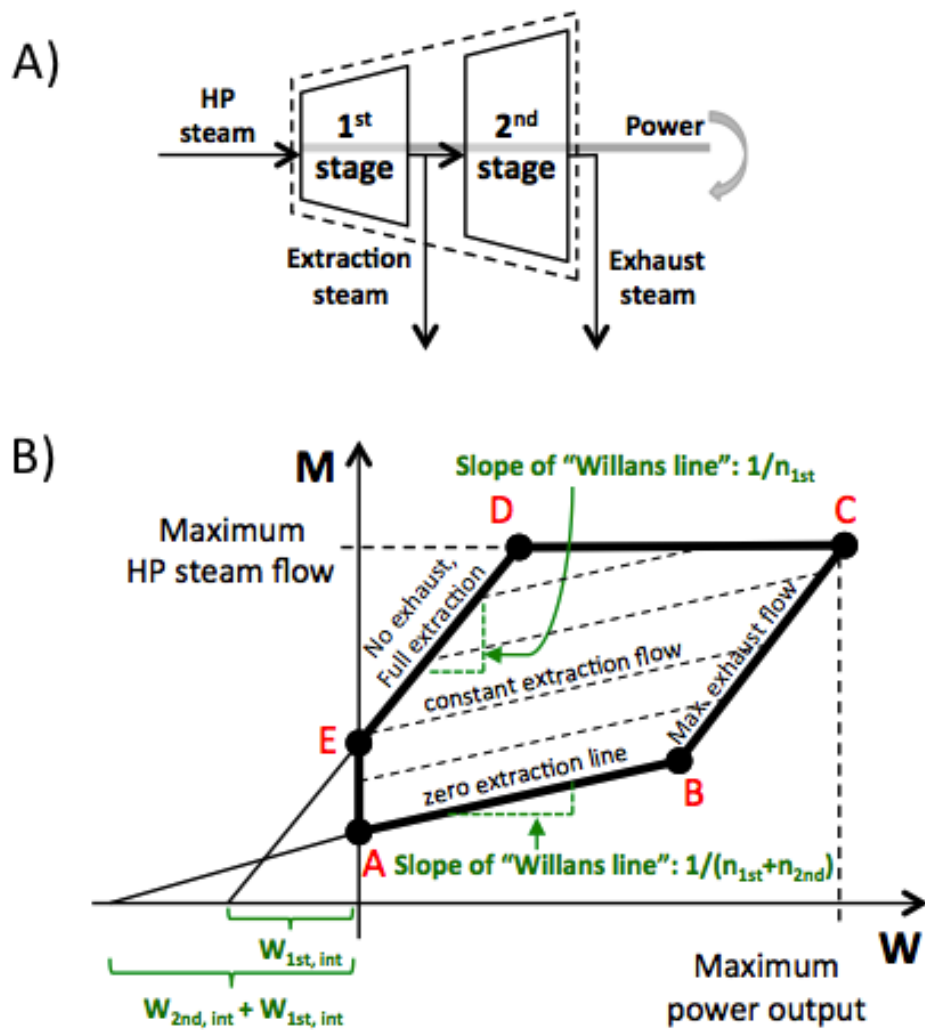


Figure 4: A: Conceptual representation of a multi-stage steam turbine, here: 2-stage with extraction. B: Willans line relationship for mode “on” of the depicted multi-stage steam turbine

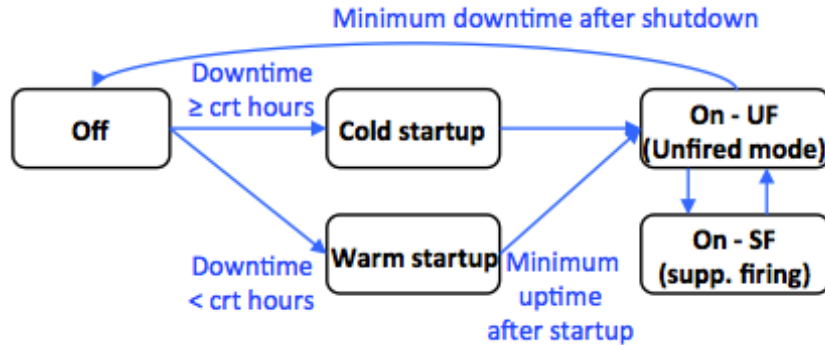


Figure 5: State graph for a gas turbine with heat recovery steam generator (HRSG).

4.1.2 Gas Turbine with Heat Recovery Steam Generator (HRSG)

Gas turbines with a heat recovery steam generator (HRSG) generate power and use the residual heat of the exhaust gas to generate steam. The steam can either be used for electricity production in a steam turbine or directly sent to a steam customer. Operating modes are similar to steam turbines: off, production and transitional modes. The state graph can be seen in Fig. 5 and will be explained in this section.

According to Aguilar et al. (2007) [31], it is possible to derive a set of linear equations that describes the part-load performance of a gas turbine with a HRSG. The produced power can be related with the produced steam in three conceptual steps. First, the relationship between fuel input and power production for part-load performance can be described with a linear function, similar to the Willans line. Second, the part-load exhaust flow has to be determined. It is important to note that the exhaust flow depends on the control mode for air regulation (no, low, medium and high) that the gas turbine is operating in. The control modes have in common that the relationship between fuel input and exhaust flow can be described again with a linear equation. Third, assuming that the operating conditions for the HRSG are given, the heat recovered from the part-load exhaust flow can be calculated.

4.1.2.1 HRSG modes: unfired and supplementary firing There are two main modes of HRSG operation: unfired and supplementary fired. The difference is that in the supplementary firing mode the exhaust gas of the gas turbine is mixed with an additional fuel and its combustion increases the available heat content in the gas, which is then used to generate steam. Note that the overall thermodynamic efficiency decreases for supplementary

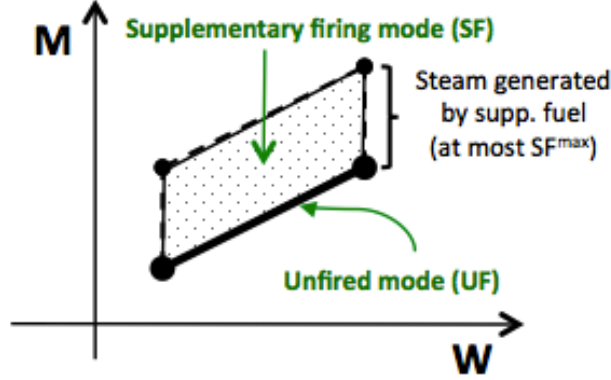


Figure 6: **Feasible region for the gas turbine with HRSG: unfired and supplementary firing mode.**

firing due to the fact that the generated heat is only used in the steam turbines to generate power.

It is possible to derive a linear equation for the total generated steam depending on the exhaust heat and the heat of the supplementary fuel, which is burnt in the supplementary firing mode (Aguilar et al., 2007 [31]). Therefore, the feasible region (for two utilities, electricity and HP steam) for the unfired mode can be specified with a linear equation. It is represented by its two extreme points at minimum and maximum power production as depicted in Fig. 6. The feasible region for supplementary firing is the area above that line, where the heat output can be boosted by at most SF_{GT}^{max} , the maximum heat generated by supplementary firing.

Additionally, the fuel consumption of the gas turbine GT has to be calculated according to the following equation:

$$fuel_{GT,on}^h = \alpha_{GT} Pr_{GT,el}^h + \beta_{GT} \quad \forall h \in H \quad (9)$$

If supplementary firing is activated, the additional fuel consumption has to be included:

$$fuel_{GT,SF}^h = \alpha_{GT,SF} (Pr_{GT,HP}^h - (\gamma_{GT} Pr_{GT,el}^h + \epsilon_{GT})) \quad \forall h \in H \quad (10)$$

4.1.3 Boiler

A boiler burns fuel and creates high pressure steam, which is then used to feed the steam turbines of the CHP plant. Operating modes for a boiler can be classified as: off, transition and production, whereas production modes

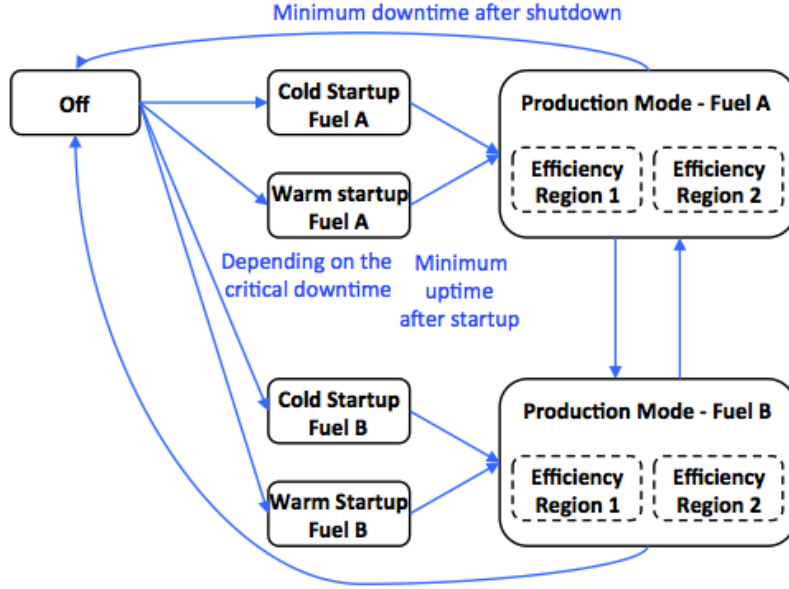


Figure 7: **State graph for a boiler with multiple fuels and different efficiency regions.**

can be distinguished by the fuel used. The state graph for a boiler can be found in Fig. 7 and is explained below.

The feasible region is defined for HP steam and the relationship between the HP steam output and the fuel consumption has to be established for all available fuels. We use a linear model, similar to the ones by Varbanov et al. (2004) [30] and Aguilar et al. (2007) [31], which can account for variations in boiler efficiency. The model has a constant conversion ratio $\alpha_{c,fl}$ based on the net heating value of fuel fl and a constant heat loss term $\beta_{c,fl}$ for boiler $c \in BL$. Note that if fuel blending is possible, an operating mode has to be introduced that captures the net heating values of the multiple fuels based on fuel composition.

$$fuel_{c,fl}^h = \alpha_{c,fl} Pr_{c,on}^h + \beta_{c,fl} \quad \forall c \in BL \subset C, fl \in FL \subset M, h \in H \quad (11)$$

In fact, two observations justify the use of such a model. First, empirical data shows that the efficiency levels off above 50% load and varies only little (Aguilar et al., 2007 [31]). Second, the same data suggests that nonlinearity in boiler efficiency is less dominant for large boilers (only 1% deviation) such as industrial cogeneration boilers. Furthermore, it is also possible to avoid low-efficiency production of steam by setting the minimum steam production rate e.g. at 50% load.

Alternatively, the feasible region of operation for fuel fl can be subdivided into load ranges that we call sub-modes $sm \in SM_{c,m}$ (for mode m of component c). In other words, we apply a piece-wise linearization of the boiler efficiency (Agha et al., 2010 [16]; Dvorak and Havel, 2012 [40]). We introduce the sub-modes sm in constraints (2) - (7) such that each feasible region is defined for $\tilde{y}_{c,m,sm}^h$ and a disjunction over $sm \in SM_{c,m}$ is added:

$$\sum_{sm \in SM_{c,m}} \tilde{y}_{c,m,sm}^h = y_{c,m}^h \quad \forall c \in BL \subset M, m \in M_c, h \in H \quad (12)$$

4.2 Logic constraints for mode transitions

The switching behavior between modes of each equipment can best be visualized with a state graph as shown in the previous section. For each equipment, we need to include the set of logic constraints that fully describes the state graph. In the following, we will present these logic constraints and focus on obtaining a good formulation in terms of tightness in the LP relaxation.

4.2.1 Switch variables constraints

We introduce the binary transitional variable $z_{c,m,m'}^h$, which is true if and only if a transition from mode m to mode m' at component c occurs from time step $h - 1$ to h . As shown in Mitra et al. (2012) [60], the logic relationship that couples $z_{c,m,m'}^h$ with the binary variables that indicate the mode of each equipment ($y_{c,m}^h$) can be modeled with the following set of equality constraints:

$$\sum_{m' \in M_c} z_{c,m',m}^h = y_{c,m}^h \quad \forall c \in C, h \in H, m \in M_c \quad (13)$$

$$\sum_{m' \in M_c} z_{c,m,m'}^h = y_{c,m}^{h-1} \quad \forall c \in C, h \in H, m \in M_c \quad (14)$$

4.2.1.1 Reformulation that eliminates self-transition variables If the self-transition variables $z_{c,m,m}^h$ are not required in the further modeling, e.g. for costs of self-transitions, they can be eliminated by taking the difference of equation (13) and (14). At the same time, the number of constraints is reduced.

$$\sum_{m' \in M_c} z_{c,m',m}^h - \sum_{m' \in M_c} z_{c,m,m'}^h = y_{c,m}^h - y_{c,m}^{h-1} \quad \forall c \in C, h \in H, m \in M_c \quad (15)$$

For a component c with only two states, on and off, only one $y_{c,m}^h$ exists since the disjunction $y_{c,on}^h + y_{c,off}^h = 1$ allows to eliminate $y_{c,off}^h$. Then, constraint (15) reduces to:

$$z_{c,off,on}^h - z_{c,on,off}^h = y_{c,on}^h - y_{c,on}^{h-1} \quad \forall c \in C, h \in H \quad (16)$$

Equation (16) is widely known from the standard unit commitment formulation (Arroyo and Conejo, 2000 [51]). Therefore, constraints (13)-(14), and constraint (15), respectively, can be seen as a generalization of equation (16).

4.2.2 Forbidden Transitions

Since the original logic relationship $(y_{c,m}^{h-1} \wedge y_{c,m'}^h) \Leftrightarrow z_{c,m,m'}^h \quad \forall c, m, m', h$ (from which constraints (13)-(14) were derived in Mitra et al. (2012) [60]) implies $\neg(y_{c,m}^{h-1} \wedge y_{c,m'}^h) \Leftrightarrow \neg z_{c,m,m'}^h \quad \forall c, m, m', h$, it is sufficient to fix $z_{c,m,m'}^h$ to zero for transitions that are not allowed (denoted by the set DAL):

$$z_{p,m,m'}^h = 0 \quad \forall (p, m, m') \in DAL, \forall h \in H \quad (17)$$

4.2.3 Minimum Stay Constraint

It was shown in the state graphs of the previous section that restrictions apply, which force the equipment to stay in a certain mode once a transition occurs, e.g. minimum uptimes or minimum downtimes. More formally, a component c has to stay a minimum time $K_{c,m,m'}^{min}$ in mode m' after a transition from mode m .

In the context of the unit commitment problem, Rajan and Takriti (2005) [53] propose a formulation for the modeling of minimum up- and downtimes. They prove that their formulation is a perfect formulation in the sense that it resembles the convex hull if the integrality conditions on the binary variables are relaxed. Hedman et al. (2009) [50] compare different formulations for minimum up/downtime and confirm their findings. We generalize their formulation with the transitional variables $z_{c,m,m'}^h$ in the following way, with MS being the set of transitions m to m' of component c with a minimum stay relationship:

$$y_{c,m'}^h \geq \sum_{\theta=0}^{K_{c,m,m'}^{min}-1} z_{c,m,m'}^{h-\theta} \quad \forall (c, m, m') \in MS, \forall h \in H, \quad (18)$$

It is interesting to note that the resulting formulation is also known in the lot-sizing problem to model the minimum run length of batches (Wolsey and Belvaux, 2001 [67]).

4.2.4 Pre-defined sequence of modes

During transitions, it is possible that the switching behavior of a component c can be described with a pre-defined sequence of modes, with a residence time specified for each mode. An example can be found during start-up procedures: first, the component c goes into the start-up mode and stays there $K_{c,off,startup}$ hours. Exactly after $K_{c,off,startup}$ hours, the component switches from the start-up mode to the production mode. In other words, the minimum stay time $K_{c,m,m'}^{min}$ is also the maximum stay time.

4.2.4.1 Transitional Mode Constraints An implication of a pre-defined sequence of modes is that transitions within the sequence are coupled. For this purpose, let $(c, m, m', m'') \in Seq$ be the set of transitions from mode m to mode m'' , which require the plant to stay in the transitional mode m' for a certain specified time $K_{c,m,m'}^{min}$, as defined before. The following constraint is proposed by Mitra et al. (2012) [60]:

$$z_{c,m,m'}^{h-K_{c,m,m'}^{min}} - z_{c,m',m''}^h = 0 \quad \forall (c, m, m', m'') \in Seq, \forall h \in H \quad (19)$$

As a consequence, the number of independent transitional binary variables can be further reduced. Pre-solve routines implemented in MILP solvers like CPLEX automatically detect the dependent binary variables and remove them.

4.2.4.2 Modification of the minimum stay constraint (18) Another implication is that the inequality constraint (18) for the minimum stay relationship becomes an equality constraint:

$$y_{c,m'}^h = \sum_{\theta=0}^{K_{c,m,m'}^{min}-1} z_{c,m,m'}^{h-\theta} \quad \forall (c, m, m') \in Seq, \forall h \in H, \quad (20)$$

4.2.5 State-dependent transitions

If the allowed transitions from a mode m to m' depend on the timing of previous transitions, we have to restrict the available transitions in hour h accordingly. One example is the dependence of the availability of start-up sequences depending on the downtime. A warm startup can be performed if the component c was shut down less hours ago than the critical downtime crt_c . If the component c was shut down more than crt_c hours ago, the warm startup is not available.

More generally, if the transition $z_{c,m,m'}^h$ occurs at hour h , then the transition from mode m'' to mode m occurred within the time window $[T_{c,m,m',m''}^L, T_{c,m,m',m''}^U]$. Hence, we derive the following logic statement:

$$z_{c,m,m'}^h \Rightarrow \bigvee_{\theta=T_{c,m,m',m''}^L-1, \dots, T_{c,m,m',m''}^U} z_{c,m'',m}^{h-\theta} \quad \forall (c, m, m', m'') \in StateDep, h \in H \quad (21)$$

Using propositional logic (Raman and Grossmann, 1993 [68]) the logic statement can be reformulated with the following constraint:

$$z_{c,m,m'}^h \leq \sum_{\theta=T_{c,m,m',m''}^L-1}^{T_{c,m,m',m''}^U} z_{c,m'',m}^{h-\theta} \quad \forall (c, m, m', m'') \in StateDep, h \in H \quad (22)$$

The resulting constraint can be seen as a generalization of a formulation in Simoglou et al. (2010) [55] for cold and warm start-ups.

4.3 Ramping constraints

Each component c has restrictions regarding its ramping behavior (up and down). The ramping constraints can be described differently for production modes and for startups.

4.3.1 Load changes in production modes

The ramping constraints for load changes in a production mode can be described with the following set of constraints, where $RU_{c,m,p}$ and $RD_{c,m,p}$ are the ramping limits for up and down ramping respectively:

$$\bar{P}r_{c,m,p}^h - \bar{P}r_{c,m,p}^{h-1} \leq RU_{c,m,p} y_{c,m}^h \quad \forall c \in C, m \in M_c, p \in P, h \in H \quad (23)$$

$$\bar{P}r_{c,m,p}^{h-1} - \bar{P}r_{c,m,p}^h \leq RD_{c,m,p} y_{c,m}^h \quad \forall c \in C, m \in M_c, p \in P, h \in H \quad (24)$$

Note that $RU_{c,m,p}$ and $RD_{c,m,p}$ are specified for the steam flowrates in $[mass/\Delta h]$ and for power in $[MW/\Delta h]$, where Δh is the chosen time discretization (e.g. one hour).

4.3.2 Pre-defined trajectories during start-ups

Nowadays, major equipment manufacturers such as Siemens and GE emphasize the ability of fast start-ups in order to cope with the flexibility in electricity pricing (Emberger et al., 2005 [69]; Jacobs and Schneider, 2009 [63]). These developments are enabled through equipment modifications and the deployment of modern control algorithms such as nonlinear model predictive control (NMPC). An example for a NMPC model used for the fast startup of a combined heat and power plant can be found in Lopez-Negrete

et al. (2012) [70]. A NMPC model can also be used to calculate the optimal startup trajectory offline. If the profile is known a priori as a sequence of output values $F_{c,m,m',p}^{def,h-\theta+1}$, it can be included in the optimization as a pre-defined trajectory during the startup, as shown by Simoglou et al. (2010) [55].

$$\bar{P}r_{c,m',p}^h = \sum_{\theta=h-K_{m,m'}+1}^h z_{c,m,m'}^\theta F_{c,m,m',p}^{def,h-\theta+1} \quad \forall (c, m, m') \in Trajectory, h \in H \quad (25)$$

Note that the trajectory might differ for each pre-computed start-up sequence (cold, warm), and a trajectory could be also included for a shutdown sequence.

4.4 Mass balances

The individual components of the plant are connected by steam pipes. The flows from component c at steam level p to component c' at steam level p' are summarized in the set $PIPES(c, p, c', p')$ and have an associated variable $F_{c,p,c',p'}^h$. We enforce a mass balance for each component c , using the steam mass flow through component c , $Pr_{c,p}^h$, which in turn is constrained by equations (2)-(7):

$$\sum_{(c',p') \in PIPES(c,p,c',p')} F_{c',p',c,p}^h - \sum_{p' \in STL} Pr_{c,p'}^h = 0 \quad \forall (c, p) \in IN, h \in H \quad (26)$$

$$Pr_{c,p}^h - \sum_{(c',p') \in PIPES(c',p',c,p)} F_{c,p,c',p'}^h = 0 \quad \forall (c, p) \in OUT, h \in H \quad (27)$$

In the previous equations, the set STL is a subset of P and contains all steam levels. IN and OUT describe at which steam levels p the component c has an inlet or outlet stream, respectively. The mixing at each steam level p is described with the following equation, where $\tilde{F}_{cust,p}^h$ is the amount of product p sent to the chemical park and $\tilde{F}_{vent,p}^h$ is the amount of steam vented:

$$\sum_{(c',p') \in PIPES(c',p',c,p)} F_{c',p',c,p}^h - \sum_{(c',p') \in PIPES(c,p,c',p')} F_{c,p,c',p'}^h - \tilde{F}_{cust,p}^h - \tilde{F}_{vent,p}^h = 0 \quad \forall (c, p) \in MIX, h \in H \quad (28)$$

Note that thermal energy storages could easily be incorporated in these mass balances.

4.5 Steam Demand Constraint

We have to satisfy hourly steam demand for each pressure level (d_p^h , $p \in STL$), which is expressed with the following constraint:

$$\tilde{F}_{cust,p}^h = d_p^h \quad \forall p \in STL, h \in H \quad (29)$$

4.6 Energy Exchange with the Power Grid

For electricity, we define the auxiliary variable Δel^h which captures the deviation from the hourly electricity demand, d_{el}^h . Δel^h is split in two parts, $\Delta^+ el^h$ and $\Delta^- el^h$, which are later used in the objective function to determine the cost or revenue from the electricity sold or purchased.

$$\Delta el^h = \sum_{c \in C} Pr_{c,el}^h - d_{el}^h \quad \forall h \in H \quad (30)$$

$$\Delta el^h = \Delta^+ el^h - \Delta^- el^h \quad \forall h \in H \quad (31)$$

$$\Delta^+ el^h, \Delta^- el^h \geq 0 \quad \forall h \in H \quad (32)$$

Furthermore, the amount of power that is transferred to or from the grid might be restricted by limits imposed by the substation the CHP is connected to. We model these substation limits with the following constraint:

$$|\Delta el^h| \leq SL \quad \forall h \in H \quad (33)$$

4.7 Additional logic constraints

The framework easily allows to incorporate additional logic constraints that model interdependencies between components that go beyond steam balances. These interdependencies can be based on technical requirements (e.g. maximum parallel start-ups or shutdowns of components), operator experience or preference, or economic considerations (maximum allowed startups or shutdowns within a given time period). Furthermore, it is also possible to schedule maintenance operations. We will study the impact of the maximum allowed shutdowns (SD_c for component c) later in this paper, which can be expressed by the following constraint:

$$\sum_{h \in H, m \in M_c} z_{c,m,off}^h \leq SD_c \quad \forall c \in C \quad (34)$$

4.8 Participation in reserve markets

As pointed out by Thorin et al. (2005) [38], it is possible to provide operating reserve based on the difference between maximum and current generation

levels. Especially in the context of the integration of intermittent renewable energy sources, reserve markets play an important role and economic benefits can be realized if the CHP plant participates in reserve markets (Lund et al., 2012 [20]). In this paper, we do not include the participation in reserve markets but our model can easily be augmented with additional constraints if desired. We refer to the papers by Thorin et al. (2005) [38] and Simoglou et al. (2010) [55] for formulations that can potentially be included.

4.9 Objective Function

The objective function maximizes the profit over the total time horizon. Note that $e_{ext}^{+,h}$ and $e_{ext}^{-,h}$ are the external electricity prices for sales of surplus electricity and purchase of electricity from the grid, respectively. Commonly, these two prices are the same.

$$\max \textit{profit} = \textit{rev}_{const} - \textit{cost} + \sum_h \Delta^+ e l^h e_{ext}^{+,h} - \sum_h \Delta^- e l^h e_{ext}^{-,h} \quad (35)$$

The revenue term \textit{rev}_{const} is constant and consists of two parts, steam revenue and internal electricity revenue. In the following equation, \textit{steam}_p is the price for steam at level p and e_{int}^h is the internal electricity price for hour h .

$$\textit{rev}_{const} = \sum_{h,p \in STL} d_p^h \textit{steam}_p + \sum_h d_{el}^h e_{int}^h \quad (36)$$

The cost term is calculated according to the amount of fuel burned and the number of start-ups and shutdowns:

$$\textit{cost} = \sum_{c,fl,h} \textit{fuel}_{c,fl}^h \textit{fuelprice}_{fl} + \sum_{c,h} z_{c,off,wst}^h \textit{SUW}_c + \sum_{c,h} z_{c,off,cst}^h \textit{SUC}_c + \sum_{c,h} z_{c,on,off}^h \textit{SD}_c \quad (37)$$

In (37), $\textit{fuelprice}_{fl}$ is the price of fuel fl . The costs coefficients \textit{SUW}_c , \textit{SUC}_c and \textit{SD}_c represent warm start-ups, cold start-ups and shutdowns of component c , respectively.

It is critical to have good estimates for the cost coefficients associated with startups and shutdowns. Usually, these costs consist not only of the additional fuel burnt. Moreover, it is important to also account for costs that originate from the cyclic type of operation and the potentially increased maintenance cost. Lefton et al. (1997) [71] describe how these costs can be estimated based on historical data, and Stoppato et al. (2012) [72] propose a model that considers effects of creep, thermo-mechanical fatigue, welding, corrosion and oxidation.

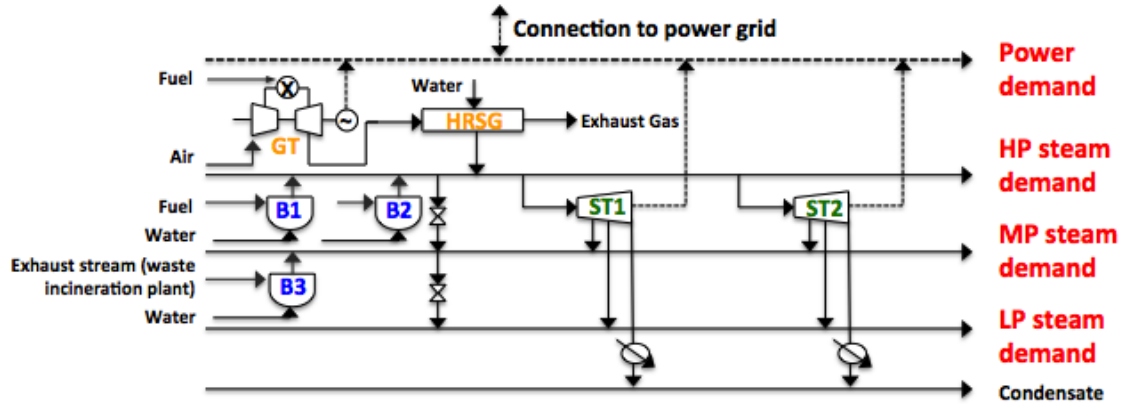


Figure 8: Flowsheet of the CHP plant

5 Case Study

We provide a case study, in which we optimize the decision-making for an industrial CHP plant that provides steam and electricity to a chemical park. Due to confidentiality reasons, we cannot disclose any information about the chemical park. In the following, we describe the layout and the data of the CHP plant and how the optimization model is set up. Furthermore, we study the impact of the optimization for different levels of utilization.

5.1 Plant description and component data

The industrial CHP plant, which has total capacity of 84.5 MW and 380 tons/hour of steam, is depicted in Fig. 8. It consists of two identical boilers (B1, B2), each can generate up to 150 tons/hour of high pressure (HP) steam. B1 and B2 are fired with natural gas. A third boiler (B3), which is a waste heat recovery boiler, generates 30 tons/hour of medium pressure (MP) steam by recovering heat from an exhaust stream that originates from the waste incineration plant of the chemical park. Additionally, up to 50 tons/hour of HP steam can be generated in the HRSG of the gas turbine (GT). The HP steam is collected in a common steam header and then sent to two steam turbines (ST1, ST2). Both turbines can extract steam at MP and LP levels and have a condensation section. Furthermore, there are letdown valves to balance the flow of steam. The data from which the feasible regions for each individual component are generated, can be found in Table 1. The operating points of the two steam turbines and their respective convex hulls are visualized in Fig. 9, where the HP steam inlet is plotted over the electricity output.

As described in section 4, the transitions between different operating

	HP	MP	LP	CON	EL
B1	75	0	0	0	0
	150	0	0	0	0
B2	75	0	0	0	0
	150	0	0	0	0
B3	0	30	0	0	0
GT	20	0	0	0	4.9
	50	0	0	0	13.6
ST1	0	41	31	37	15.8
	0	3	0	76	19.0
	0	46	36	58	24.7
	0	29	46	77	31.2
	0	0	88	53	28.9
	0	0	73	64	29.4
	0	0	70	80	34.6
ST2	0	75	75	50	31.9
	0	75	95	30	29.4
	0	95	75	30	27.3
	0	95	95	10	25.2
	0	60	60	55	28.4
	0	60	75	40	26.5
	0	75	60	40	24.9
	0	75	75	25	23.1
	0	60	60	30	19.7
	0	60	75	15	18.0
	0	75	60	15	16.5
	0	60	60	10	13.3
	0	95	75	55	36.3

Table 1: Output data for each individual plant component, from which the feasible region is created. HP steam: 111 bar, 520°C; MP steam: 21 bar, 320°C; LP: 4.5 bar, 180°C. Units: ton/hr for steam, MW for electricity.

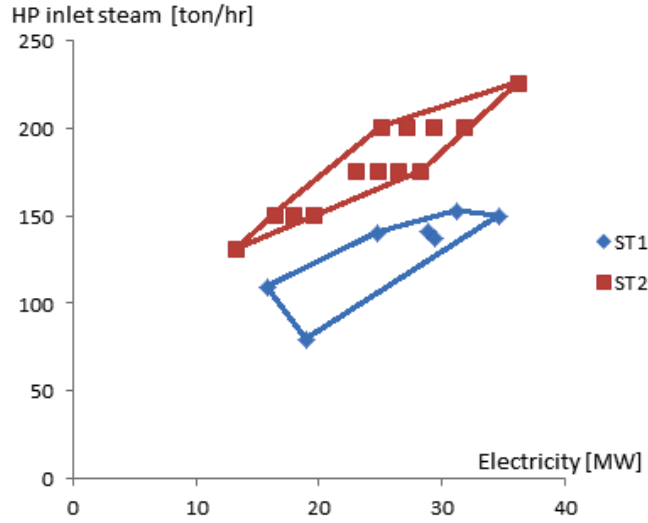


Figure 9: Operating points of the steam turbines ST1 and ST2 and their respective convex hulls.

modes are restricted. In Table 2, the requirements for minimum uptime, the warm and cold startup times are listed. Note that the critical downtime is 6 hours, after which only a cold startup can be performed. Boiler B3 cannot be shutdown, therefore, no values are reported.

	Min. uptime	Warm startup time	Cold startup time
B1	40	1	2
B2	24	1	2
B3*	-	-	-
GT	1	1	1
ST1	2	1	2
ST2	4	1	2

Table 2: Requirements for transition times for all components (in hours).

The cost data for the objective function coefficients can be found in Table 3. Note that the cost for warm and cold startups only include charges for the fuel that is consumed during the startup procedure. As noted in section 4.9, the additional cost for equipment wear and tear should be included as well based on historic plant data. Due to the lack of access to this data, we compare later in this section how shutdown restrictions impact the profit. Based on this comparison, the plant operator can assess whether a shutdown is economically feasible.

Note that due to confidentiality reasons, the reported values for variable and fixed cost coefficients in Table 3 are lumped parameters and include

conversion ratios from equations (9) and (11), and the fuel price for natural gas in equation (37). While the fixed cost coefficient for gas turbine GT is only assigned if GT is in mode “on”, the fixed cost for boilers B1 and B2 are assigned independently of the state of the equipment since the boilers are not shut down completely. Instead, the boilers are always in stand-by if no HP steam is generated and they are shut down only once per year for a major revision. Boiler B3 has no cost term since it is a waste heat recovery boiler that recovers the residual heat from an exhaust stream of the waste incineration plant of the chemical park, which is provided with no extra charge.

	Warm startup [\$]	Cold startup [\$]	Variable cost [\$/ton HP]	Fixed cost [\$/h]
B1	300	600	24.888	179.2
B2	400	800	24.872	182.784
B3*	-	-	-	-
GT	180	360	29.377	358.4
ST1	200	400	-	-
ST2	230	460	-	-

Table 3: Cost table for the individual plant components.

There is a bilateral contract between the industrial CHP plant and the consumers in the chemical park that defines the product prices for HP, MP and LP steam as well as electricity. The corresponding prices, which are used to calculate the revenue from the chemical park, can be found in Table 4. Note that these values are constant over the time horizon of one week since they are re-negotiated on a seasonal basis.

	HP [\$/ton]	MP [\$/ton]	LP [\$/ton]	EL [\$/MWh]
Product price (internal)	38.40	24.81	9.15	109.16

Table 4: Internal product prices based on a contract with the chemical plant (constant over the time horizon).

5.2 Model formulation

The feasible region for each plant component is modeled with equations (2)-(7). Note that the Willans line equation is not included explicitly, as described in section 4. The logic constraint (15) is used to link the mode variables $y_{c,m}^h$ for each plant component with the corresponding transitional variables $z_{c,m,m'}^h$. Constraint (17) enforces that forbidden transitions cannot be active. Minimum stay restrictions for transitions and uptime (Table 2)

are modeled with constraint (18). For sequence dependent transitions, such as warm and cold startups, constraints (19), (20) and (22) are employed.

The mass balance equations (26)-(28) are included, as well as constraint (29), which enforces that the steam demand is satisfied. The demand for electricity and steam at different pressure levels is specified on an hourly basis for the time horizon of one week (168 hours). We study different demand scenarios (A-H) that can be found in Table 5, which can be distinguished by the level of utilization. Note that the demand data assumes a constant demand profile for the entire week, which is due to the steady-state behavior of the associated industrial process. The electricity price forecast is assumed to be a typical week in the summer of 2008 based on PJM data (www.pjm.com) and is reported in Table 6. Constraints (30)-(32) are included to determine the amount of electricity exchanged with the grid. The calculation of the profit, which is maximized, is performed with constraints (9), (11) and (35)-(37).

The substation that the plant is connected with, can transmit the maximum amount of electricity that can be produced within the CHP plant. Therefore, no restriction on the amount of electricity is included. Furthermore, no rate-of-change restrictions are included since each component is capable of ramping from the minimum production level to the maximum production level within the given time discretization of one hour. The number of shutdowns is restricted with constraint (34), where the values for SD_c are varied within our case study. The initial state of all components is 'on'.

	EL	HP	MP	LP	CON	% of max Steam	% of max EL
A-45%	16	10	75	85	0	45%	19%
A-45%-B1ST1off	16	10	75	85	0	45%	19%
B-50%	30	30	80	80	0	50%	36%
C-61%	40	30	100	100	0	61%	47%
D-79%	40	40	120	140	0	79%	47%
E-50%	60	30	80	80	0	50%	71%
F-76%	60	50	120	120	0	76%	71%
G-84%	75	20	100	100	100	84%	89%
H-71%	70	10	140	120	0	71%	83%

Table 5: Hourly constant steam (ton/hr) and electricity demand (MWh) for the different cases. The percentages represent the level of utilization depending on the maximum steam/electricity output of the CHP plant. In case A-45%-B1ST1off, boiler B1 and steam turbine ST1 are switched off permanently due to low capacity utilization.

	Mon	Tue	Wed	Thu	Fri	Sat	Sun
1	74.47	25 73.76	49 71.59	73 71.19	97 75.49	121 72.49	145 71.68
2	61.67	26 60.81	50 59.65	74 59.56	98 62.24	122 61.22	146 58.80
3	54.24	27 54.12	51 52.42	75 52.94	99 53.82	123 51.37	147 49.84
4	50.16	28 49.50	52 48.43	76 48.94	100 48.42	124 46.39	148 44.37
5	51.65	29 50.36	53 49.03	77 50.05	101 48.97	125 45.08	149 42.73
6	60.61	30 59.69	54 58.47	78 58.17	102 57.88	126 47.26	150 43.03
7	73.33	31 75.07	55 75.26	79 73.37	103 70.76	127 48.56	151 42.95
8	78.52	32 78.90	56 76.61	80 78.01	104 77.85	128 57.43	152 50.60
9	89.19	33 88.78	57 83.83	81 85.49	105 84.63	129 73.34	153 66.56
10	106.38	34 103.88	58 95.67	82 98.56	106 99.05	130 97.70	154 86.12
11	126.38	35 120.89	59 110.56	83 113.30	107 115.40	131 116.08	155 102.67
12	142.76	36 140.41	60 126.24	84 129.73	108 131.01	132 129.90	156 121.61
13	156.82	37 153.94	61 136.10	85 138.12	109 141.74	133 141.53	157 134.27
14	170.55	38 169.68	62 148.15	86 152.34	110 154.11	134 147.10	158 140.35
15	182.34	39 184.76	63 160.21	87 164.73	111 162.69	135 155.32	159 148.37
16	199.88	40 199.18	64 173.83	88 179.33	112 177.70	136 167.39	160 159.65
17	209.06	41 208.01	65 179.00	89 186.55	113 184.50	137 171.66	161 168.15
18	199.48	42 197.97	66 173.20	90 176.83	114 171.74	138 162.44	162 162.58
19	166.29	43 159.68	67 143.20	91 146.87	115 143.34	139 139.72	163 140.37
20	146.04	44 137.65	68 122.91	92 127.28	116 126.97	140 123.53	164 125.69
21	151.89	45 141.29	69 132.37	93 134.18	117 131.61	141 131.48	165 135.32
22	130.88	46 124.22	70 116.02	94 120.52	118 116.28	142 119.18	166 119.88
23	97.82	47 93.38	71 85.15	95 88.85	119 90.41	143 93.07	167 93.74
24	84.87	48 83.82	72 79.99	96 86.48	120 82.57	144 83.19	168 83.11

Table 6: Electricity price for the given week in \$/MWh.

5.3 Results

5.3.1 Economic Impact and Physical Interpretation

We investigate the economic impact of our optimization model for different levels of utilization (cases A-H with constant demand as reported in Table 5) with different restricted versions of the model in four steps. First, the model is solved under the restriction that all components of the CHP plant operate at only one setpoint for the whole week (constant operation). Second, the production levels of the CHP plant are optimized (variable operation), while equipment shutdowns are still not allowed. Third, the model is optimized with component shutdowns allowed (1, 2 and 3 per component). Finally, fourth, the constraint on the shutdowns allowed is relaxed.

The results, which are shown in Fig. 10, clearly demonstrate that the economic performance can be improved by applying the optimization model. While the largest marginal improvement originates from varying the production levels, significant improvements can also be observed from allowing multiple shutdowns of components. For cases with lower utilization (A, B, E), the impact of allowing shutdowns is higher (up to 20 % improvements compared to the base case) compared to the cases with higher utilization (C, D, F, G, H), where mostly 5% improvements can be observed.

The improvements were realized by generating surplus electricity prices during hours of favorable prices, and by the timing of shutdowns and start-

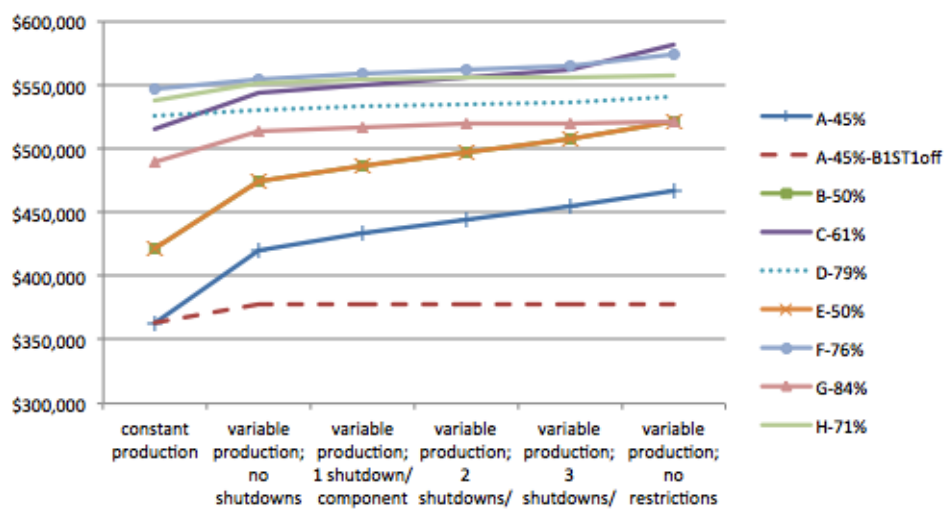
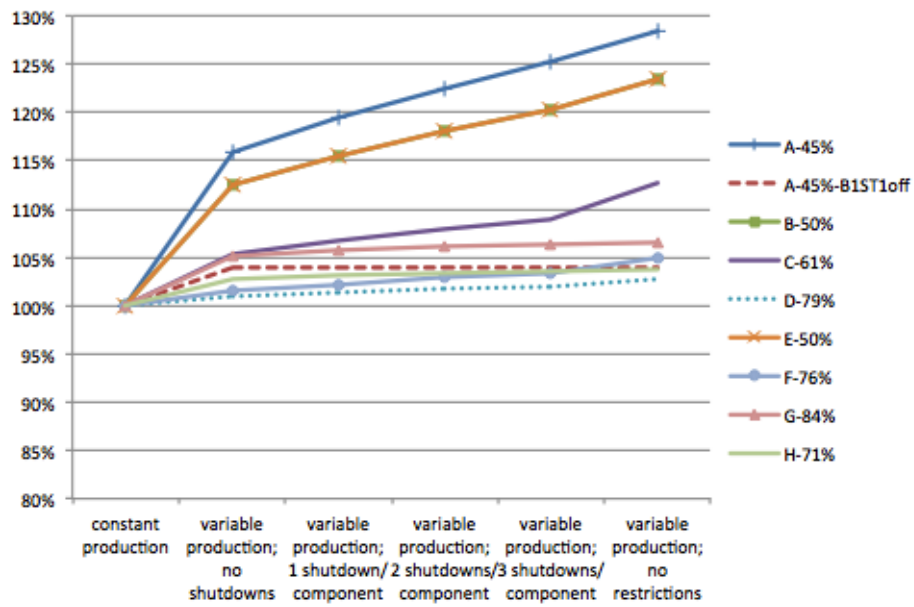


Figure 10: Results: Incremental improvements in profit for cases A-H (absolute and relative) due to shutdowns.

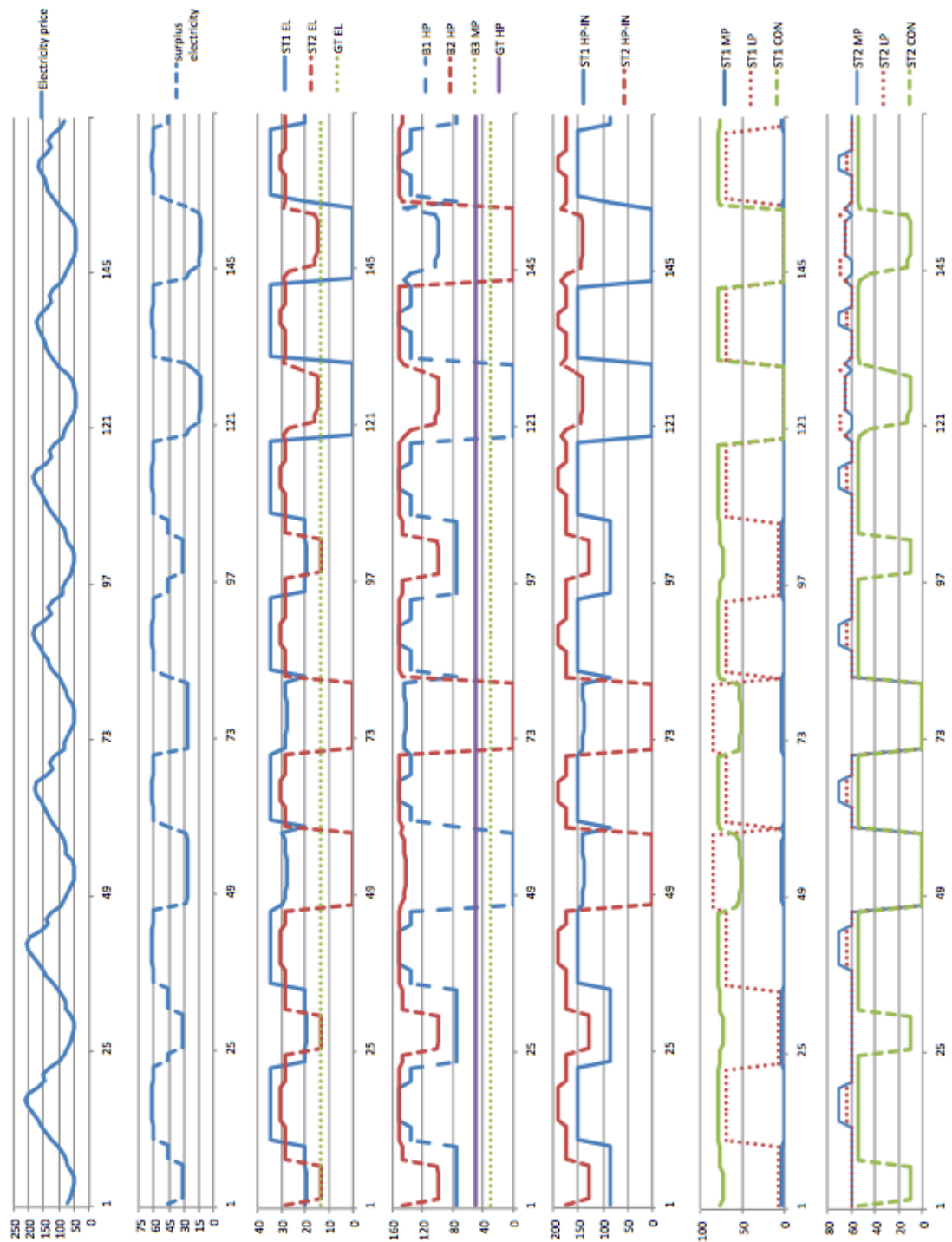


Figure 11: Case A: Results on component level (in \$/MWh for electricity price, ton/hr for steam and MWh for electricity).

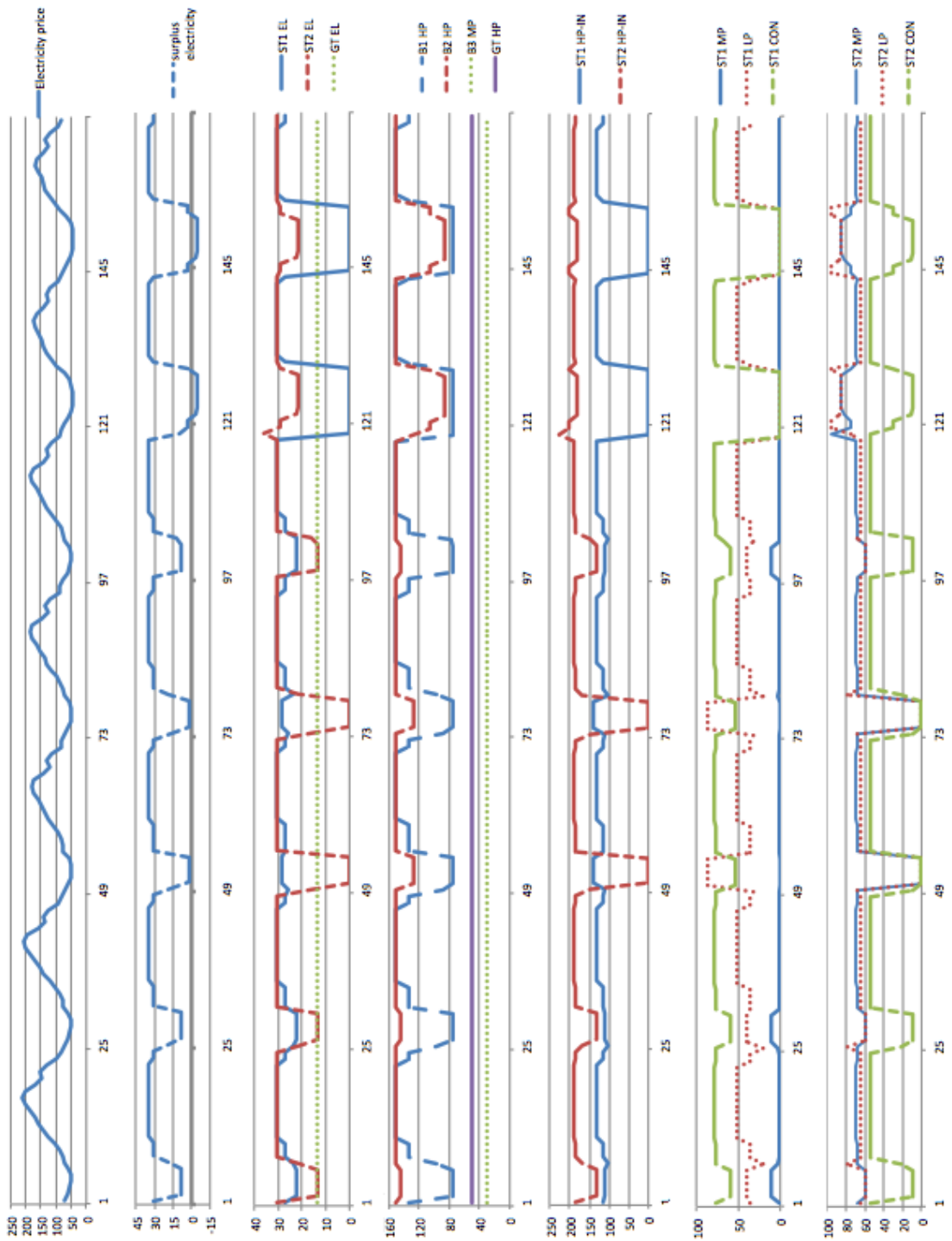


Figure 12: Case C: Results on component level (in \$/MWh for electricity price, ton/hr for steam and MWh for electricity).

ups of generation assets, while the CHP plant always satisfied the constant steam and electricity demand of the chemical park. Temporary shutdowns increase the operational profit since production is stopped when market conditions are not in favor to the production of surplus electricity. During these hours, electricity is even bought from the power grid if the electricity that is generated by expanding the HP steam according to steam demand does not cover the internal electricity demand (see e.g. case C). Additionally, it can be seen that the permanent shutdown of components (case A-B1ST1off: B1 and ST1 offline) reduces the operational flexibility in such a way that swings in electricity prices cannot be exploited to the full extent.

For two cases (A and C) with two shutdowns allowed per component, the individual flows of the components are reported in Fig. 11 and 12. It can be observed that the HP boilers B1 and B2 adjust their steam production according to the electricity prices. During peak prices, the production is at the maximum rate. In contrast, if prices are low during the night, the steam production is reduced, which is also reflected in the steam flows through ST1 and ST2. The amount of condensate is reduced, which decreases the electricity production.

If the utilization is low enough, one boiler is even shut down. Note that during the same hours one of the steam turbines has to be shut down as well due to the less amount of HP steam available. If one of the steam turbines goes offline, the extraction flows of the remaining turbine changes according to the steam demand such that only small amounts of steam have to be routed through the letdown valves. The startup procedures involve mostly cold startups, which seem to be more advantageous under the given electricity prices. The gas turbine GT operates constantly due to the associated low cost of co-generation of steam and electricity. The MP pressure boiler B3 also operate constantly since it recovers heat from the exhaust stream of the waste incineration plant of the chemical park that is provided with no cost associated.

5.3.2 Computational Statistics

The resulting optimization model is large, it has as 49,535 variables, of which 8,722 are binary, and 70,009 constraints. Despite the large size, all cases can be solved in less than 2 minutes (except case A with no restrictions, which takes about 9 minutes). The commercial solver CPLEX 12.4.0.1 was employed with default settings in GAMS 23.9.1 (Brooke et al., 2012 [73]) on a Intel i7-2600 (3.40 GHz) machine with 8 GB RAM, using a termination criterion of 0% optimality gap. The corresponding statistics can be found in Table 7. Note that the requirement of 0% gap ensures that the mathematical optimum is reached. If the solution process needs to be sped up, a small tolerance can be introduced (e.g. 0.1 %).

It can be observed that the optimization problem can be solved faster

case	constant operation	0 SD allowed	1 SD allowed	2 SD allowed	3 SD allowed	no SD restrictions
A-45%	5	5	12	38	61	526
A-45%-B1ST1off	4	4	5	6	6	6
B-50%	5	5	15	62	119	25
C-61%	5	5	26	53	40	10
D-79%	6	7	8	9	8	8
E-50%	5	5	14	54	71	25
F-50%	5	5	18	36	31	29
G-84%	5	5	9	9	10	10
H-71%	5	5	12	11	12	8

Table 7: CPU times in seconds for the investigated cases. SD is an abbreviation for shutdown, no restrict. means no restrictions for the number of shutdowns within the week.

if the utilization increases. This behavior is mainly due to the fact that an increased steam demand implies fewer alternatives for equipment shutdowns, which in turn reduces the solution space.

6 Conclusions

In this paper, we have presented a generalized mode model on a component basis for the optimal scheduling of combined heat and power plants under time-sensitive electricity prices. The model is capable of tracking the states of the components in terms of operating modes and transitional behavior, and can capture the inherent flexibility of the CHP plant. We applied the model successfully to a real-world industrial CHP plant. When compared to constant operation, the optimization model was able to improve the profit up to 5 % for higher utilization cases and up to 20 % for lower utilization cases, depending on the number of shutdowns allowed. The improvements were realized by generating surplus electricity prices during hours of favorable prices, and by the timing of shutdowns and start-ups of generation assets. Therefore, the production profiles for each component adapted to the swings in electricity prices, while the CHP plant always satisfied the steam and electricity demand of the chemical park. Despite the large size of the resulting MILP model, the problem could be solved within a few minutes to optimality. The efficient deterministic formulation we reported can serve as a basis for the development of models based on the frameworks of stochastic programming (Birge and Louveaux, 2011 [74]) or robust optimization (Ben-Tal et al., 2009 [75]), which address uncertainty in electricity price data originating e.g. from intermittent renewable energy sources.

Acknowledgments

We would like to thank the National Science Foundation for financial support under grant #1159443. We are also grateful to Joachim Eisenberg for the fruitful discussions on the case study and the data provided.

Nomenclature

Sets

- C (index c): The set of components
- $MIX \subseteq C$: The set of mixers, that is used to formulate the mass balance for each steam level
- $M(c)$ (index m), abbreviated as M_c : The set of modes, depending on component c
- $SM(c, m)$ (index sm), abbreviated as $SM_{c,m}$: The set of sub-modes, for mode m depending on component c (e.g. operating regions with different efficiencies for boilers)
- $I(c, m)$ (index i), abbreviated as I : The set of extreme points that relate to mode m of component c
- P (index p): The set of products, for the CHP plant it is $\{HP, MP, LP, CON, EL\}$
- $STL \subseteq P$: The set of steam levels, $\{HP, MP, LP, CON\}$
- FL (index fl): The set of fuels.
- $PIPES(c, p, c', p'), IN(c, p), OUT(c', p')$: Indicate whether there is a steam pipe connection from component c at steam level p to component c' at steam level p' .
- H (index h): The set of hours of a week in the operational model
- $Seq(c, m, m', m'')$: The set of possible transitions for component c from mode m to a production mode m'' with the transitional mode m' in between
- $MS(c, m, m')$: The set of transitions for component c from mode m to another mode m' with a minimum stay relationship
- $DAL(c, m, m')$: The set of disallowed transitions from mode m to mode m' of component c
- $StateDep(c, m, m', m'')$: Depending on the transition from mode m'' to m , the transition from mode m to m' of component c is restricted

- $Trajectory(c, m, m')$: The set of transitions from mode m to m' of component c for which a pre-computed trajectory exists

Variables

Binary variables

- $y_{c,m}^h$: Determines whether component c operates in mode m in hour h
- $Z_{c,m,m'}^h$: Indicates whether there is a transition from mode m to mode m' at component c from hour $h - 1$ to h

Continuous variables

- $\bar{P}_{c,m,g}^h$: Production amount of product g in mode m at component c in hour h
- $P_{c,g}^h$: Total production of product g at component c in hour h
- $\lambda_{c,m,i}^h$: Variable for the convex combination of slates i to describe the feasible region of the component c of mode m in hour h
- $fuel_{c,m}^h$: Fuel consumption of component c in mode m
- $\Delta el^h, \Delta^+ el^h, \Delta^- el^h$: Difference between produced electricity and electricity demand in hour h
- $F_{c,p,c',p'}^h$: Flow from component c at steam level p to component c' at steam level p' in hour h
- $F_{cust,p}^h$: Steam at steam level p that is sent to the chemical park in hour h
- $F_{vent,p}^h$: Steam at steam level p that is vented in hour h
- $profit$: Objective function variable
- $cost$: Operational cost associated to fuel consumption, startups and shutdowns

Parameters

- $\alpha_{c,m}, \beta_{c,m}, \gamma_{c,m}, \epsilon_{c,m}$: Fitting parameters related to fuel consumption for mode m of component c
- $e_{ext}^{+h}, e_{ext}^{-h}$: External electricity prices in hour h for sales (+) and purchases (-)
- e_{int}^h : Internal electricity prices in hour h

- $x_{c,m,i,p}$: Extreme points of the convex hull of the feasible regions
- $\tilde{M}_{c,m,p}$: BigM constant for bounds on production for component c (i.e. max. production of product p in mode m)
- $K_{c,m,m'}^{min}$: Number of hours component c has to stay in mode m' after a transition from mode m
- $RU_{c,m,p}$: Maximum rate of change (up) for product p at component c in mode m
- $RD_{c,m,p}$: Maximum rate of change (down) for product p at component c in mode m
- d_p^h : Hourly demand for product p in hour h . It is the demand for the steam at different pressure levels and the demand for electricity.
- SF_c^{max} : Maximum amount of steam generated by supplementary firing for a gas turbine with HRSG, $c \in GT$.
- crt_c : Critical downtime of component c , after which a warm startup is impossible
- $T_{c,m,m',m''}^L, T_{c,m,m',m''}^U$: Lower and upper bounds of a time window according to set $StateDep$
- $F_{c,m,m',p}^{def,h-\theta+1}$: Defined output of component c in mode m for product p , θ hours after a transition from mode m to m'
- SL : Substation limit for the amount of power that is exchanged with the power grid
- SD_c : Number of allowed shutdowns during the time horizon for component c
- rev_{const} : Constant revenue from internal steam and electricity sales
- $fuelprice_{fl}$: Fuel price for fuel fl
- $steam_p$: Internal steam price for product p (at steam level STL)
- SUW_c : Warm startup cost of component c
- SUC_c : Cold startup cost of component c
- SD_c : Shutdown cost of component c

References

- [1] Madlener, R.; Schmid, C., “Combined heat and power generation in liberalised markets and a carbon-constrained world,” *GAIA - Ecological Perspectives for Science and Society*, vol. 12, pp. 114–120, 2003.
- [2] Kerr, T., “Combined Heat and Power, Evaluating the benefits of greater global investment,” 2008. International Energy Agency report.
- [3] Shipley, A.; Hampson, A.; Hedman, B.; Garland, P.; Bautista, P., “Combined Heat and Power, Effective Energy Solutions for a Sustainable Future,” 2008. Report by Oak Ridge National Laboratory for the U.S. Department of Energy.
- [4] The Press and Information Office of the Federal German Government, “Growth and Responsibility in the World Economy,” 2007. Summit Declaration (7 June 2007).
- [5] The European Parliament, “Directive 2004/8/EC of the European Parliament and of the Council of 11 February 2004 on the promotion of cogeneration based on a useful heat demand in the internal energy market and amending Directive 92/42/EEC,” 2004. 21/02/2004.
- [6] German Federal Ministry for the Environment, Nature Conservation and Nuclear Safety, “The Integrated Energy and Climate Programme of the German Government, background paper as of December 2007,” 2007. <http://www.bmu.de/english/climate/downloads/doc/40589.php>, accessed 04/03/2012.
- [7] German Federal Ministry of Justice, “Gesetz für die Erhaltung, die Modernisierung und den Ausbau der Kraft-Wärme-Kopplung (KWKG-Novelle),” 2009. 1. Januar 2009.
- [8] The European Commission, eurostat, “Combined heat and power generation, % of gross electricity generation,” 2012.
- [9] Federal Reserve, “Industrial Production and Capacity Utilization,” 2011. March 2011 release, accessed on 10/21/2011.
- [10] German Chemical Industry Association, “Chemical Parks: Industry Landscaping a la Germany,” *Chemical Engineering Progress*, vol. 107, no. 10, 2011.
- [11] Lewe, T.; Disteldorf, H., “Future challenges for chemical sites, A.T. Kearney study,” 2007.
- [12] Lewe, T.; Schroeter, I., “Onsite Service Providers in the Chemical Industry, A.T. Kearney study,” 2010.

- [13] Wassick, J.M., “Enterprise-wide optimization in an integrated chemical complex,” *Computers & Chemical Engineering*, vol. 33, pp. 1950–1963, 2009.
- [14] Samad, T.; Kiliccote, S., “Smart Grid Technologies and Applications for the Industrial Sector,” *Computers & Chemical Engineering*, vol. in press, 2012.
- [15] Todd, D, Caufield, M., Helms, B., Starke M., Kirby B., Kueck, J., “Providing Reliability Services through Demand Response: A Preliminary Evaluation of the Demand Response Capabilities of Alcoa Inc.,” tech. rep., U.S. Department of Energy, 2009.
- [16] Agha, M.; They, R.; Hetreux, G.; Hait, A.; Le Lann, J.M., “Integrated production and utility system approach for optimizing industrial unit operations,” *Energy*, vol. 35, pp. 611–627, 2010.
- [17] Christidis, A.; Koch, C.; Pottel, L.; Tsatsaronis G., “The contribution of heat storage to the profitable operation of combined heat and power plants in liberalized electricity markets,” *Energy*, vol. 41, pp. 75–82, 2012.
- [18] Cole, W.J.; Powell, K.M.; Edgar, T.F., “Optimization and Control of Thermal Energy Storage Systems,” *Reviews in Chemical Engineering*, 2012.
- [19] Wille-Haussmann B.; Erge T.; Wittwer, C., “Decentralised optimisation of cogeneration in virtual power plants,” *Solar Energy*, vol. 84, no. 4, pp. 604 – 611, 2010. International Conference CISBAT 2007.
- [20] Lund, H.; Andersen, A.N.; Ostergaard, P.A.; Mathiesen, B.V.; Connolly, D., “From electricity smart grids to smart energy systems - A market operation based approach and understanding,” *Energy*, vol. 42, pp. 96–102, 2012.
- [21] Nishio, M.; Itoh, J.; Shiroko, K.; Umeda, T., “Thermodynamic approach to steam and power system design,” *Industrial & Engineering Chemistry Process Design and Development*, vol. 19, pp. 306–312, 1980.
- [22] Petroulas, T.; Reklaitis, G. V., “Computer-aided synthesis and design of plant utility systems,” *AIChE Journal*, vol. 30, pp. 69–78, 1984.
- [23] Marechal, F.; Kalitventzeff, B., “Process integration: Selection of the optimal utility system,” *Computers & Chemical Engineering*, vol. 22, pp. 149–156, 1998.
- [24] Papoulias, S.A.; Grossmann, I.E., “A structural optimization approach in process synthesisI. Utility systems,” *Computers & Chemical Engineering*, vol. 7, pp. 695–706, 1983.

- [25] Colmenares, T. R.; Seider, W. D., "Synthesis of utility system integrated with chemical process," *Industrial & Engineering Chemistry Research*, vol. 28, pp. 84–93, 1989.
- [26] Bruno, J.C.; Fernandez, F.; Castells F.; Grossmann, I.E., "MINLP Model for Optimal Synthesis and Operation of Utility Plants," *Transaction of the Institution of Chemical Engineers*, vol. 76, pp. 246–258, 1998.
- [27] Iyer, R.; Grossmann, I.E., "Synthesis and operational planning of utility systems for multiperiod operation," *Computers & Chemical Engineering*, vol. 22, pp. 979–993, 1998.
- [28] Willans, P.W., "Economy Trials of a Non-Condensing Steam-Engine: Simple, Compound and Triple. (Including Tables and Plate at Back of Volume)," *Minutes of the Proceedings*, vol. 93, pp. 128–188, 1888.
- [29] Mavromatis, S.P.; Kokossis, A.C., "Conceptual optimisation of utility networks and operational variations - I. Targets and level optimisation," *Chemical Engineering Science*, vol. 53, pp. 1585–1608, 1998.
- [30] Varbanov, P.S.; Doyle, S.; Smith, R., "Modelling and Optimization of Utility Systems," *Chemical Engineering Research and Design*, vol. 82, pp. 561–578, 2004.
- [31] Aguilar, O.; Perry, S.J.; Kim, J.-K.; Smith, R., "Design and Optimization of Flexible Utility Systems Subject to Variable Conditions Part 1: Modelling Framework," *Chemical Engineering Research and Design*, vol. 85, pp. 1136–1148, 2007.
- [32] Micheletto, S.R.; Carvalho, M.C.A.; Pinto, J.M., "Operational optimization of the utility system of an oil refinery," *Computers & Chemical Engineering*, vol. 32, pp. 170–185, 2008.
- [33] Luo, X.; Zhang, B.; Chen, Y.; Mo, S., "Operational planning optimization of multiple interconnected steam power plants considering environmental costs," *Energy*, vol. 37, pp. 549–561, 2012.
- [34] Seeger, T.; Verstege, J., "Short Term Scheduling in Cogeneration Systems," *Proc. of the 17th Power Industry Computer Application Conference*, pp. 106–112, 1991. May 7-10 1991, Baltimore.
- [35] Salgado, F.; Pedrero, P., "Short-term operation planning on cogeneration systems: A survey," *Electric Power Systems Research*, vol. 78, pp. 835–848, 2008.
- [36] Makkonen S.; Lahdelma, R., "Non-convex power plant modelling in energy optimisation," *European Journal of Operational Research*, vol. 171, no. 3, pp. 1113 – 1126, 2006.

- [37] Tina, G.M.; Passarello, G., “Short-term scheduling of industrial cogeneration systems for annual revenue maximisation,” *Energy*, vol. 42, pp. 46–56, 2012.
- [38] Thorin, E; Brand, H.; Weber, C., “Long-term optimization of cogeneration systems in a competitive market environment,” *Applied Energy*, vol. 81, pp. 152–169, 2005.
- [39] Marshman, D.J.; Chmelyk, T.; Sidhu, M.S.; Gopaluni, R.B.; Dumont, G.A., “Energy optimization in a pulp and paper mill cogeneration facility,” *Applied Energy*, vol. 87, pp. 3514–3525, 2010.
- [40] Dvorak, M.; Havel, P., “Combined heat and power production planning under liberalized market conditions,” *Applied Thermal Engineering*, vol. in press, 2012.
- [41] Ashok, S.; Banerjee, R., “Optimal Operation of Industrial Cogeneration for Load Management,” *IEEE Transactions on Power Systems*, vol. 18, pp. 931–937, 2003.
- [42] Yusta, J.M.; De Oliveira-De Jesus P.M.; Khodr, H.M., “Optimal energy exchange of an industrial cogeneration in a day-ahead electricity market,” *Electric Power Systems Research*, vol. 78, pp. 1764–1772, 2008.
- [43] Velasco-Garcia, P.; Varbanov, P.S.; Arellano-Garcia H.; Wozny, G., “Utility systems operation: Optimisation-based decision making,” *Applied Thermal Engineering*, vol. 31, pp. 3196–3205, 2011.
- [44] Pantelides, C. C., “Unified Frameworks for the Optimal Process Planning and Scheduling,” *Proceedings on the Second Conference on Foundations of Computer Aided Operations*, pp. 253–274, 1994.
- [45] Dotzauer, E.; Holmstrom, K.; Ravn, H.F., “Optimal Unit Commitment and Economic Dispatch of Cogeneration Systems with a Storage,” *13th PSCC Proceedings*, pp. 738–744, 1999. Trondheim, Norway, June 1999.
- [46] Rong, A.; Hakonen, H.; Lahdelma, R., “A dynamic regrouping based sequential dynamic programming algorithm for unit commitment of combined heat and power systems,” *Energy Conversion and Management*, vol. 50, pp. 1108–1115, 2009.
- [47] Sandou, G.; Font, S.; Tebbani, S.; Hiretand, A.; Mondon, C., “Short term optimization of cogeneration systems considering heat and electricity demands,” *15th Power Systems Computation Conference, Lige, Belgium*, 2005.
- [48] Padhy, N.P., “Unit Commitment - A Bibliographical Survey,” *IEEE Transactions on Power Systems*, vol. 19, pp. 1196–1205, 2004.

- [49] Sen, S.; Kothari, D.P., “Optimal thermal generating unit commitment: a review,” *International Journal of Electrical Power & Energy Systems*, vol. 20, pp. 443–451, 1998.
- [50] Hedman, K.W.; O’Neill R.P.; Oren, S.S., “Analyzing Valid Inequalities of the Generation Unit Commitment Problem,” *Power Systems Conference and Exposition, 2009. PSCE ’09. IEEE/PES*, pp. 1–6, 2009.
- [51] Arroyo, J.M.; Conejo, A.J., “Optimal Response of a Thermal Unit to an Electricity Spot Market,” *IEEE Transactions on Power Systems*, vol. 15, pp. 1098–1104, 2000.
- [52] Carrion, M.; Arroyo, J.M., “A Computationally Efficient Mixed-Integer Linear Formulation for the Thermal Unit Commitment Problem,” *IEEE Transactions on Power Systems*, vol. 21, pp. 1371–1378, 2006.
- [53] Rajan, D.; Takriti, S., “Minimum Up/Down Polytopes of the Unit Commitment Problem with Start-Up Costs,” tech. rep., IBM Research Division, 2005.
- [54] Ostrowski, J; Anjos, M.F.; Vannelli, A., “Tight Mixed Integer Linear Programming Formulations for the Unit Commitment Problem,” *IEEE Transactions on Power Systems*, vol. 27, pp. 39–46, 2012.
- [55] Simoglou, C.K.; Biskas, P.N.; Bakirtzis, A.G., “Optimal Self-Scheduling of a Thermal Producer in Short-Term Electricity Markets by MILP,” *IEEE Transactions on Power Systems*, vol. 25, pp. 1965–1977, 2010.
- [56] Cohen, A.I.; Ostrowski, G., “Scheduling units with multiple operating modes in unit commitment,” *IEEE Transactions on Power Systems*, vol. 11, pp. 497–503, 1996.
- [57] Lu, B.; Shahidehpour, M., “Short-Term Scheduling of Combined Cycle Units,” *IEEE Transactions on Power Systems*, vol. 19, pp. 1616–1625, 2004.
- [58] Lu, B.; Shahidehpour, M., “Unit Commitment with Flexible Generating Units,” *IEEE Transactions on Power Systems*, vol. 20, pp. 1022–1034, 2005.
- [59] Liu, C.; Shahidehpour, M.; Li, Z.; Fotuhi-Firuzabad, M., “Component and Mode Models for the Short-Term Scheduling of Combined Cycle Units,” *IEEE Transactions on Power Systems*, vol. 24, pp. 976–990, 2009.
- [60] Mitra, S; Grossmann, I. E.; Pinto, J. M.; Arora, N., “Optimal Production Planning under Time-sensitive Electricity Prices for Continuous Power-intensive Processes,” *Computers & Chemical Engineering*, vol. 38, pp. 171–184, 2012.

- [61] Balas, E., “Disjunctive Programming and a Hierarchy of Relaxations for Discrete Optimization Problems,” *SIAM Journal on Algebraic and Discrete Methods*, vol. 6, pp. 466–486, 1985.
- [62] Drbal, L.F.; Boston, P.G.; Westra, K.L., *Power Plant Engineering*. Springer, 1996.
- [63] Jacobs, J.A.; Schneider, M., “Cogeneration Application Considerations,” 2009. GE Energy report.
- [64] Barber, C.B.; Dobkin D.P.; Huhdanpaa, H., “The quickhull algorithm for convex hulls,” *ACM TRANSACTIONS ON MATHEMATICAL SOFTWARE*, vol. 22, no. 4, pp. 469–483, 1996.
- [65] The MathWorks Inc., “MATLAB 7.10.0.499 (R2010a),” 2010.
- [66] Christof, T.; Lobel, A., “The PORTA manual page v. 1.4.1,” tech. rep., ZIB, Berlin, 1997.
- [67] Belvaux, G.; Wolsey, L.A., “Modelling Practical Lot-Sizing Problems as Mixed-Integer Programs,” *Management Science*, vol. 47, no. 7, pp. 993–1007, 2001.
- [68] Raman, R.; Grossmann, I.E., “Modeling and Computational Techniques for Logic Based Integer Programming,” *Computers & Chemical Engineering*, vol. 18, p. 563, 1993.
- [69] Emberger, H.; Schmid, E., Gobrecht, E., “Fast Cycling Capability for New Plants and Upgrade Opportunities,” 2005. Siemens Power Generation report.
- [70] Lopez-Negrete, R.; DAmato, F.J.; Biegler, L.T.; Kumar, A., “Fast nonlinear model predictive control: Formulation and industrial process applications,” *Computers & Chemical Engineering*, vol. in press, 2012.
- [71] Lefton, S.A.; Besuner, P.M.; Grimsrud, G.P., “Understand what it really costs to cycle fossil-fired units,” *Power*, vol. 141, 1997. March/April 1997.
- [72] Stoppato, A.; Mirandola, A.; Meneghetti, G.; Lo Casto, E., “On the operation strategy of steam power plants working at variable load: Technical and economic issues,” *Energy*, vol. 37, pp. 228–236, 2012.
- [73] Brooke, A.; Kendrick, D.; Meeraus, A., “GAMS: A Users Guide, Release 23.9.1,” *The Scientific Press, South San Francisco*, 2012.
- [74] Birge, J.R.; Louveaux, F., *Introduction to Stochastic Programming*. Springer Series in Operations Research, Springer, 2011.

- [75] Ben-Tal, A.; El Ghaoui, L.; Nemirovski, A., *Robust Optimization*. Princeton Series in Applied Mathematics, Princeton University Press, 2009.